

A Computational Approach to Hedging Credit Valuation Adjustment in a Jump-Diffusion Setting

Thomas van der Zwaard^{a,b,*}, Lech A. Grzelak^{a,b}, Cornelis W. Oosterlee^{a,c}

^a*Delft Institute of Applied Mathematics, Delft University of Technology, Delft, the Netherlands*

^b*Rabobank, Utrecht, the Netherlands*

^c*CWI - National Research Institute for Mathematics and Computer Science, Amsterdam, the Netherlands*

Abstract

This study contributes to understanding Valuation Adjustments (xVA) by focussing on the dynamic hedging of Credit Valuation Adjustment (CVA), corresponding Profit & Loss (P&L) and the P&L explain. This is done in a Monte Carlo simulation setting, based on a theoretical hedging framework discussed in existing literature. We look at CVA hedging for a portfolio with European options on a stock, first in a Black-Scholes setting, then in a Merton jump-diffusion setting. Furthermore, we analyze the trading business at a bank after including xVAs in pricing. We provide insights into the hedging of derivatives and their xVAs by analyzing and visualizing the cash-flows of a portfolio from a desk structure perspective. The case study shows that not charging CVA at trade inception results in a guaranteed loss. Furthermore, hedging CVA is crucial to end up with a stable trading strategy. In the Black-Scholes setting this can be done using the underlying stock, whereas in the Merton jump-diffusion setting we need to add extra options to the hedge portfolio to properly hedge the jump risk. In addition to the simulation, we derive analytical results that explain our observations from the numerical experiments. Understanding the hedging of CVA helps to deal with xVAs in a practical setting.

Keywords: computational finance, dynamic hedging, Credit Valuation Adjustment (CVA), Merton jump-diffusion, counterparty credit risk (CCR), xVA hedging

1. Introduction

Since the 2007-2008 global financial crisis, financial institutions have been required to apply and report Valuation Adjustments (xVAs) for over-the-counter (OTC) derivatives and hedge the associated risks. These adjustments to the risk-neutral price of a derivative account for previously neglected risks that were revealed during the crisis. Credit Valuation Adjustment (CVA), corresponding to Counterparty Credit Risk (CCR), was the first of many xVAs. CVA volatility is one of the major drivers behind the large losses observed during the crisis. Linear contracts¹ are no longer linear when CCR is included in the valuation. Hence, not including CCR in pricing results in an incorrect hedging policy. Next, xVA pricing evolved with various other xVAs, see [1, 15] for more information. Calculating the increasing number of xVAs is computationally challenging, and has attracted significant academic and corporate interest.

The first literature on xVA pricing appeared before and during the crisis [14, 19, 29]. To date, several books have addressed the topic [1, 7, 15]. There are three streams in literature on xVA pricing, all describing the mathematical problem in different ways. First of all, there is the Monte Carlo approach where the xVA is expressed as an expectation. A set of risk factors is simulated in a Monte Carlo engine, after which the future exposures that contribute to the xVA

^{*}Corresponding author at Delft Institute of Applied Mathematics, TU Delft, Delft, the Netherlands.

Email addresses: T.vanderZwaard@tudelft.nl (Thomas van der Zwaard), L.A.Grzelak@tudelft.nl (Lech A. Grzelak), C.W.Oosterlee@cwi.nl (Cornelis W. Oosterlee)

The views expressed in this paper are the personal views of the authors and do not necessarily reflect the views or policies of their current or past employers.

¹Linear contracts/instruments have contractual cash-flows that are a linear function of the underlying.

metrics are evaluated along the simulated paths [2, 3, 8, 9, 10]. The Monte Carlo approach allows for scalable computations. Hence, this type of method is typically implemented by banks. Second, there is the PDE approach that aims to solve the xVA PDE directly [5, 13]. Dimensionality is one of the downsides of this approach, though low-dimensional non-linear problems can be treated highly accurately. Last, there is the BSDE approach, where the main purpose is to get accurate Greeks [20, 21, 24, 25, 28]. This may be non-trivial in a regression based Monte Carlo approach. Literature on xVA has focussed on deriving the mathematical pricing equations, as well as addressing the computational challenges that arise when solving these pricing equations. In our work, we closely examine xVA pricing and hedging. We focus on the dynamic hedging of CVA, where we study the cash-flows of a portfolio from a desk structure perspective. This results in an improved understanding of the CVA hedging mechanics. We show that the CVA in the portfolio needs to be hedged to end up with a stable trading strategy.

The trading strategy is a combination of all trading positions with a counterparty and the corresponding hedging strategy [2, 3]. A wealth account [11] is connected to this trading strategy, it tracks the total wealth of the trading strategy over time. This is a cash account that accrues interest. Bielecki and Rutkowski formalized this framework [28]. The generic trading strategy formulation provides a useful framework to analyze exchanges of assets and cash. Furthermore, the generic formulation is useful for the hedging of xVAs. We provide numerical examples and insights in a Monte Carlo simulation setting, starting in the Black-Scholes world.

The constant volatility is one of the known shortcomings of the Black-Scholes model. The resulting flat implied volatility is in clear contrast with the market's implied volatility smile. To properly manage this smile risk, several streams of modelling have emerged. Among these approaches are the local volatility models (e.g., Dupire [4], Derman and Kani [12]) and the stochastic (local) volatility models (e.g., Heston [27], Hagan *et al.* [22]). Although these models fit in the generic hedging framework, we choose to focus on jump-diffusion models, which exhibit heavy tails in the distribution of stock returns and fit well with the jump patterns observed for stocks. Jump-diffusion models extend the Black-Scholes model with independently distributed jumps driven by a Poisson process. Typical choices of jump size distributions are a double exponential distribution, Kou [26], or normal distributed jumps, Merton [23]. We choose to work with the latter. Further research on the Merton jump-diffusion model has been on calibrating the model and hedging the jump risk that partially drives option prices under this model [6, 16].

Therefore, after studying the dynamic hedging of CVA in a Black-Scholes setting, we do the same in a Merton jump-diffusion setting. The numerical analysis is performed by means of a Monte Carlo simulation. In addition, we examine the impact of defaults on the portfolio. The Profit and Loss of the trading strategy is examined to assess the hedge's performance. We show that, for a portfolio of European options, not including CVA in the pricing results in a guaranteed loss on average. Hence, we interpret CVA as a fair compensation for the credit risk of the counterparty. Charging CVA to the client at trade inception overcomes the guaranteed loss at maturity. CVA can be treated as a cash amount, however, this ignores the dependencies of the CVA on the market variables. After including the CVA hedge in the strategy, we assess the impact of jumps in the underlying stock on the portfolio. In particular, we find that in the context of CVA, the jump risk can be mitigated to a large degree by adding extra hedging instruments to the strategy. Rather than merely performing a simulation, we also derive analytic results to understand and explain our numerical observations.

This paper is organized as follows. In Section 2 we provide background information on Profit and Loss, which is used to examine the outcome of the hedging strategies. In Section 3 we introduce the trading strategy and the corresponding wealth account. Next, the numerical simulation of the future market states and results of the various hedging strategies will be addressed in Sections 4 and 5 respectively. Finally, the work is concluded in Section 6.

2. Profit and Loss

Profit and Loss (P&L) is a financial institution's income statement. This is an officially reported number that summarizes the change in *Mark-to-Market* (MtM) value over a period of time, normally one business day. During this period, the institution examines which part of the change in MtM can be attributed to market moves and other predefined effects, such

as the passing of time. This process is also called P&L *attribution*, or P&L *explain*, which explains the impact of the daily market movements on the value of the portfolio. The goal is to verify that the modelled risk factors satisfactorily explain the change in portfolio value. The P&L explain process runs after the closing of every business day, so it is a backward looking measure. Typically, the variance between two consecutive days is also examined.

A financial institution wants to explain the P&L as well as possible. Hence the residual P&L, which from now on we address as P&L *unexplained*, should be as small as possible. Yet explaining all P&L is insufficient, as extreme numbers that are completely explained are also undesirable. Therefore, institutions put thresholds/limits on both P&L and P&L unexplained at a portfolio level, where the thresholds depend on the portfolio composition. In addition to these P&L limits, market risk limits on particular risk types are in place for both traders and portfolios. The aim of these market risk limits is to make sure the trading activities remain within the institution's predefined risk appetite and that exposure to certain market drivers is bounded. This naturally limits the P&L as well. The portfolios are not always entirely flat in terms of risk, as in practice it is not feasible to rebalance the hedge daily, for example due to transaction costs. Furthermore, having a flat portfolio is not always the goal as this may be a way to express a view on the market. In practice, the residual risk of a portfolio is being monitored.

For xVAs a separate explain process exists, which is analogous to the one for the MtM value. Limits on market risk drivers, P&L and P&L unexplained are present.

In literature the following approaches to P&L explain can be found [1, 18]:

1. A Taylor-based explain process where the partial derivatives of the instrument V with respect to *market data* γ_i are used to explain the difference in $V(t_{k-1})$ and $V(t_k)$, $t_{k-1} < t_k$.² In other words,

$$V(t_k) - V(t_{k-1}) = \frac{\partial V}{\partial t} \Big|_{t_{k-1}} dt + \mathcal{A}(t_{k-1}) + \text{P\&L}_U(t_k), \quad (2.1)$$

$$\mathcal{A}(t_{k-1}) = \sum_{i=1}^n \frac{\partial V}{\partial \gamma_i} \Big|_{t_{k-1}} d\gamma_i + \frac{1}{2} \sum_{i=1}^n \sum_{j=1}^n \frac{\partial^2 V}{\partial \gamma_i \partial \gamma_j} \Big|_{t_{k-1}} d\gamma_i d\gamma_j.$$

The left hand side of Equation (2.1) is P&L(t_k). $\text{P\&L}_U(t_k)$ is the unexplained P&L. The remaining terms can be interpreted as $\text{P\&L}_E(t_k)$, i.e., the explained P&L.

2. In the second approach, the *theta effect* $\frac{\partial V}{\partial t} \Big|_{t_{k-1}} dt$, is neglected and we are only interested in the change of value V in the interval $[t_{k-1}, t_k]$ as a result of movements in the underlying market data γ_i .³ Let $V(t, t) = V(t, \gamma(t))$ denote value V at time t with a set of market data $\gamma(t)$. In other words,

$$V(t_{k-1}, t_k) - V(t_{k-1}, t_{k-1}) = \mathcal{A}(t_{k-1}) + \text{P\&L}_U(t_k). \quad (2.2)$$

The left hand side of Equation (2.2) is P&L(t_k), and the $\mathcal{A}(t_{k-1})$ term is $\text{P\&L}_E(t_k)$. The effect of ignoring the theta should not be too large, as P&L explain is a daily process, but the size of the effect will depend on the portfolio composition. This method considers instrument values at the same date, and the difference in value is caused by a perturbed market data set.

3. Another approach is a high-level attribution using effects to explain the P&L in a consecutive manner.⁴ Before starting the explain process, a list of effects is composed, which are applied one-by-one. After applying an effect, the portfolio is revalued and the difference is attributed to the particular effect. These changes will be permanent, so when

²Green refers to this as “risk-based explain” [1, Section 21.1.4]. Andersen and Piterbarg use the term “second order P&L predict” [18, Section 22.2.1].

³Green refers to this as “orthogonal explain” [1, Section 21.1.4]. Andersen and Piterbarg use the term “perturbed market data approach” [18, Section 22.1.5].

⁴Green refers to this as “step-wise explain” [1, Section 21.1.4]. Andersen and Piterbarg use the term “bump and do not reset” type of P&L explain, a.k.a. the “waterfall explain” [18, Section 22.2.1].

applying a new effect, the old effects stay in place. This implies that cross-effects are introduced, which cannot be allocated properly, as well as an order dependence on the effects. Yet this approach should yield similar results as the previous ones. Examples of the effects used in the P&L attribution can be: time decay (including holiday effects, carry effects as well as shifts in market data), market data changes (IR / FX / inflation / bonds / credit), turns, fixings, and trade closing.

When a financial institution observes jumps in P&L, these are investigated. Real-world jumps are typically caused by trade insertions or cancellations (captured via the theta term), rather than by underlying market movements. Though theta contributions will be present in practice, they are not relevant for our discussion, which focusses on the effect of market movements on the P&L of a portfolio. Hence we use the orthogonal explain approach as per Equation (2.2), which makes use of perturbed market data. Here we can simply take the next day's market data as the perturbed market data.

3. Hedging framework

We start with a risk-neutral pricing framework, where we consider the various contributions to the price of a derivative. Using the standard replicating portfolio argument [7], the price of a derivative is equivalent to the price of a replicating portfolio containing other securities.

We define a trading strategy as a combination of positions in a set of available trading instruments, accompanied by the hedging positions in hedging instruments, which mitigate the market risk associated with the positions in the trading instruments. We assume that the short-selling of all assets is possible. In practice, hedges do not necessarily mitigate all the market risk, but certain limits are placed per market risk factor on a portfolio level. A trader will make sure that the exposure of a portfolio to certain risk factors will remain below these predefined thresholds by taking the necessary positions in market instruments. Here we will assume that all the market risk is always reduced by the dynamic hedging strategy, i.e., we choose the hedging positions that together replicate the risk profile of the trading positions as good as possible.

The *trading strategy* $\Pi(t)$ is generically defined for N *trading instruments* $V_i(t)$ in which *trading positions* $\zeta_i(t)$ are taken, which are assumed to be exogenously provided. Analogously, we consider M *hedging instruments* $H_i(t)$ in which *hedging positions* $\eta_i(t)$ are taken. The trading strategy $\Pi(t)$ is then summarized as follows:

$$\Pi(t) = \sum_{i=1}^N \zeta_i(t) V_i(t) + \sum_{i=1}^M \eta_i(t) H_i(t). \quad (3.1)$$

We start in a Black-Scholes setting, where European options are considered for the sake of clarity and ease of computation. However, the generic formulation allows for much more flexibility, for example, for the case of a large portfolio of interest rate swaps. The underlying interest rate risks are then eliminated by taking hedging positions in the par instruments used to build the underlying yield curve(s) that are in turn required to value the portfolio of interest rate swaps.

Define the *cash-flows* for the trading and hedging instruments respectively by $c_{i,j}^T(t)$ and $c_{i,j}^H(t)$, denoting the time t value of the j -th cash-flow paid at time T_j , corresponding to respectively instruments V_i and H_i , which in total generate respectively n_i and m_i cash-flows. We then define the time t value of the cumulative cash-flows corresponding to instrument V_i and H_i respectively as

$$C_i^T(t) = \sum_{j=1}^{n_i} \zeta_i(T_j) c_{i,j}^T(t) \mathbb{1}_{\{T_j \leq t\}}, \quad C_i^H(t) = \sum_{j=1}^{m_i} \eta_i(T_j) c_{i,j}^H(t) \mathbb{1}_{\{T_j \leq t\}}, \quad (3.2)$$

which is to be interpreted as the quantity representing all cash-flows paid up and till time t , taking into account the time value of money, $B(t)$, being the *bank account*. This is the solution of $dB(t) = r(t)B(t)dt$, where $B(t_0) = 1$ and with *risk-free rate* $r(t)$.

In parallel with the trading strategy $\Pi(t)$, we define a *wealth process* $w(t)$ that represents the total wealth realized over time, obtained by summing up all the profits and losses over time. There are two sources for changes in wealth: one is the rebalancing of positions in instruments, the other results from cash-flows associated with the various instruments. We assume that $V_i(t)$ and $H_i(t)$ denote the value after exchange of all cash-flows at time t . For example, if a cash-flow takes place at date t , the values $V_i(t)$ and $H_i(t)$ do not contain the value of this cash-flow. Rebalancing the trading positions, and consecutively the hedging positions, takes place after the exchange of cash-flows. The wealth is a cash amount that accrues interest over time at the risk-free rate. At this stage we do not distinguish between different levels of interest rate for paying and receiving interest.

At time t_0 , the wealth will be composed of the cost to enter the positions in all instruments, including any potential cash-flows taking place at t_0 :

$$w(t_0) = -\Pi(t_0) + \sum_{i=1}^N C_i^T(t_0) + \sum_{i=1}^M C_i^H(t_0). \quad (3.3)$$

The rebalancing of the trading and hedging positions is denoted by $d\zeta_i(t)$ and $d\eta_i(t)$ respectively. We write the following (recursive) expression for the wealth at $t_0 \leq t_{k-1} < t_k$:

$$\begin{aligned} w(t_k) = w(t_{k-1}) \frac{B(t_k)}{B(t_{k-1})} - \sum_{i=1}^N B(t_k) \int_{t_{k-1}}^{t_k} \frac{V_i(u)}{B(u)} d\zeta_i(u) + \sum_{i=1}^N B(t_k) \int_{t_{k-1}}^{t_k} \frac{dC_i^T(u)}{B(u)} \\ - \sum_{i=1}^M B(t_k) \int_{t_{k-1}}^{t_k} \frac{H_i(u)}{B(u)} d\eta_i(u) + \sum_{i=1}^M B(t_k) \int_{t_{k-1}}^{t_k} \frac{dC_i^H(u)}{B(u)}. \end{aligned} \quad (3.4)$$

The first term in Equation (3.4) is the wealth at the previous point in time t_{k-1} that has accrued interest. This is followed by the re-balancing and cash-flows of respectively the trading and hedging instruments.

The continuous time formulation from Equation (3.4) is discretized in time $t_0 < t_1 < \dots < t_{k-1} < t_k \dots < t_K$:⁵:

$$\begin{aligned} w(t_k) \approx w(t_{k-1}) \frac{B(t_k)}{B(t_{k-1})} - \sum_{i=1}^N V_i(t_k) d\zeta_i(t_k) + \sum_{i=1}^N dC_i^T(t_k) \\ - \sum_{i=1}^M H_i(t_k) d\eta_i(t_k) + \sum_{i=1}^M dC_i^H(t_k). \end{aligned} \quad (3.5)$$

In this context, the initial wealth from Equation (3.3) remains valid. Furthermore, t_K is the final time at which either all trading instruments have matured, or at which all positions are closed. We keep the positions in trading and hedging instruments constant over a time interval $(t_{k-1}, t_k]$. The terms $dC_i^T(t_k)$ and $dC_i^H(t_k)$ respectively represent the trading and hedging instruments' cash-flows present in time interval $(t_{k-1}, t_k]$:

$$dC_i^T(t_k) = \sum_{j=1}^{n_i} \zeta_i(T_j) c_{i,j}^T(t_k) \mathbb{1}_{\{t_{k-1} < T_j \leq t_k\}}, \quad dC_i^H(t_k) = \sum_{j=1}^{n_i} \eta_i(T_j) c_{i,j}^H(t_k) \mathbb{1}_{\{t_{k-1} < T_j \leq t_k\}}. \quad (3.6)$$

Strategy (3.1) is by design *self-financing*, i.e., there is no cash in- and/or outflow during the lifetime of the strategy. In other words, $\Pi(t) + w(t) = 0$ holds on average. At t_0 we assume that any funding required to set up the trading strategy is obtained from the internal Treasury department.

3.1. Output metrics

Now that the trading strategy $\Pi(t)$ and wealth $w(t)$ are defined, we define several output metrics to evaluate the performance of the trading strategy. In a perfect world, the self-financing constraint $\Pi(t) + w(t) = 0$ holds on average for all $t_k \in [t_0, t_K]$, i.e.,

⁵For a generic function $f(\cdot)$ we define $df(t_k) = f(t_k) - f(t_{k-1})$

$\mathbb{E}_{t_0} [\Pi(t_k) + w(t_k)] = 0$. In particular, we are interested in this condition at final time t_K , where all open positions are closed such that $\Pi(t_K) = 0$. So, we evaluate the *expected terminal wealth*: $\mathbb{E}_{t_K} [w(t_0)]$. Assuming that one can continuously rebalance the hedging positions, the terminal wealth should be zero on average.

In addition to the terminal wealth, we also examine P&L. The relevant market information at time t is represented by $\gamma(t)$ and we rewrite $V_i(t)$ as follows: $V_i(t, t) = V_i(t, \gamma(t))$. This allows us to price product V_i at time t with a set of market data $\gamma(t)$. In a similar fashion, we write $H_i(t, t) = H_i(t, \gamma(t))$. Define the following P&L quantities corresponding to trading strategy (3.1):

$$P\&L_T(t_k) = \sum_{i=1}^N \zeta(t_{k-1}) [V_i(t_{k-1}, t_k) - V_i(t_{k-1}, t_{k-1})], \quad (3.7)$$

$$P\&L_H(t_k) = \sum_{i=1}^M \eta(t_{k-1}) [H_i(t_{k-1}, t_k) - H_i(t_{k-1}, t_{k-1})], \quad (3.8)$$

$$P\&L_P(t_k) = P\&L_T(t_k) + P\&L_H(t_k). \quad (3.9)$$

$P\&L_T$ in Equation (3.7) is the P&L generated by the trading positions. When the hedging quantities $\eta(t)$ are based on sensitivities of the trading positions, $P\&L_H$ in Equation (3.8) can be seen as a first-order P&L explain. By choosing the same instruments for hedging as for the daily P&L explaining process, we are in fact looking at how well the hedging strategy is able to explain changes in value of the trading strategy as a result of changes in the market data.

The residual risk, after combining trading and hedging positions, is represented by $P\&L_P$ in Equation (3.9). As the hedge is constructed to eliminate all desired sources of randomness, the daily change portfolio value is automatically equal to the $P\&L_P$, i.e., we can rewrite $P\&L_P$ from Equation (3.9) by means of Equations (3.7) and (3.8):

$$P\&L_P(t_k) = \Pi(t_{k-1}, t_k) - \Pi(t_{k-1}, t_{k-1}). \quad (3.10)$$

We then use the orthogonal P&L attribution process from Equation (2.2) to assess which portion of the residual risk can be explained. Note the absence of cash-flows in this discussion. This is because we want to treat cash-flows in a consistent manner, such that only the market movements are attempted to be explained.

4. Market simulation

The hedging framework from Section 3 will be used in a numerical simulation setting to assess Valuation Adjustments and the hedging thereof. The starting point of the numerical analysis is choosing a portfolio of trading instruments and the corresponding hedging instruments. The economic value of a trading instrument is the combination of the risk-free value and Valuation Adjustments, where we choose to look at CVA only. We consider only European options for the trading instruments. DVA turns out to be trivial for this portfolio composition, so DVA is ignored in the analysis. CVA computations require the following two main components: market exposure and default probability. The former is introduced in Section 4.1, the latter is discussed here directly.

We model the jump-to-default by a Poisson process $X_{\mathcal{P}}(t)$ with constant hazard rate $\lambda(t) = \xi_{\mathcal{P}}$, i.e. a homogenous Poisson process.⁶ The deterministic hazard rate (e.g., constant or piece-wise constant) implies that credit events⁷ are independent of the interest rates and deterministic recovery rates. In addition, assume that the *recovery rate* R is deterministic.

⁶ To gain some intuition on how this Poisson processes works, look at its expected value $\mathbb{E}[X_{\mathcal{P}}(t)] = \xi_{\mathcal{P}}t$, which is the expected number of events in a time interval with length t . So say we have an interval $[0, T]$ of length T where we expect one event every $2T$, then we must set $\xi_{\mathcal{P}} = \frac{1}{2T}$.

⁷ A credit event is considered to be the first event of a Poisson counting process which occurs at some random time τ with probability $\mathbb{P}(X_{\mathcal{P}}(\tau + dt) - X_{\mathcal{P}}(\tau) | X_{\mathcal{P}}(\tau) = 0)$, i.e., the probability of default in interval $[\tau, \tau + dt]$ conditional on survival until time τ .

Survival probability $SP(t, T)$ is the probability that the counterparty will survive until time T , conditional on survival till time t :

$$SP(t, T) = \mathbb{E}_t \left[\exp \left\{ - \int_t^T \lambda(s) ds \right\} \right] = \exp \left\{ - \int_t^T \lambda(s) ds \right\} = e^{-\xi_P(T-t)}.$$

A credit curve is the credit-analogue of the yield curve, where we do not extract discount factors but survival probabilities from the curve. In a market implied setting, survival probabilities $SP(t_0, T)$ are extracted from the market using quotes of highly standardized CDSs. For CVA calculations we require knowledge about the *probability of default* $PD(t, T)$ of a counterparty in a certain time interval $[t, T]$. The probability of default is related to the survival probability: $PD(t, T) = 1 - SP(t, T)$.

We choose to hedge all the market risk introduced by the risk-free value and CVA corresponding to the trading instruments. We do not consider the credit risk component introduced by the CVA. In Section 4.2 we look in more detail at the setup of the trading strategy.

4.1. Model-free European option exposures

Given a call option V that runs from t_0 till maturity t_K , we create a grid of *monitoring dates* $t_0 < t_1 < \dots < t_k \dots < t_K$ at which we compute *exposures*. The following convenient result can easily be derived for the *discounted expected positive exposure* (EPE) of a call/put option:

$$EPE(t_0, t_k) = V(t_0). \quad (4.1)$$

Using the result from Equation (4.1) in the formula for CVA, assuming no *Wrong Way Risk (WWR)*, yields:

$$\begin{aligned} CVA(t_0) &= (1 - R) \sum_{k=1}^K EPE(t_0, t_k) PD(t_{k-1}, t_k) \\ &= (1 - R) \sum_{k=1}^K V(t_0) PD(t_{k-1}, t_k) \\ &= (1 - R)V(t_0) PD(t_0, t_K). \end{aligned} \quad (4.2)$$

The results in Equations (4.1) and (4.2) are model-free up to the level how $V(t)$ is computed.⁸

4.2. Simulation framework

For our trading instruments we choose a constant long unit position (i.e., buy) in a European call option $V_1(t)$, i.e., $N = 1$ and $\zeta_1(t) = 1 \forall t$.⁹ The option is assumed to be an OTC deal where the underlying asset $S(t)$ is a third-party asset, i.e., $S(t)$ is not the asset of the option seller. This implies the absence of WWR, meaning we assume that the creditworthiness of the option seller and buyer and the underlying asset move independently. In addition, we assume a constant credit curve over time, i.e., no stochasticity for the credit is used. Furthermore, we assume the option has a cash-settled payoff. The market risk of the option is hedged by buying/selling the underlying stock from/to an exchange, i.e., $M = 1$ and $H_1(t) = S(t)$:

$$\Pi(t) = V_1(t) + \eta_1(t)S(t), \quad (4.3)$$

where $\eta_1(t)$ depends on a model chosen by the financial institution. Hedging positions $\eta_1(t)$ are rebalanced on a daily basis. We assume no dividends are paid, though they can easily be added to the framework in the form of cash-flows. The trading instrument will generate one cash-flow,

⁸CVA is in essence a compound option on the value of a portfolio. A compound option refers to an option on an option. Say that we consider a portfolio of a single option, then the max function in the expected exposure in the CVA formula makes the CVA a compound option.

⁹This reverse Black-Scholes hedge is an academic setup, as buying a call option and hedging the delta risk is not what one usually encounters. However, for illustrative purposes this particular setting is chosen.

namely the payoff at maturity in case the option is in the money and the counterparty has not defaulted.

The trading instruments $V_i(t)$ can represent the risk-neutral value, which corresponds to the case without Counterparty Credit Risk (CCR). On the other hand, it can also represent the economic value, which is the sum of the risk-neutral value and xVAs that are taken into account, and corresponds to the case where CCR is taken into account, i.e.,

$$\begin{cases} V_1(t) &:= V(t), & \text{(the case without CCR)} \\ V_1(t) &:= V(t) - \text{CVA}(t) & \text{(the case with CCR)} \\ &= V(t) (1 - (1 - R) \text{PD}(t, t_K)), \end{cases} \quad (4.4)$$

where for the case with CCR we used Equation (4.2). Recall that $V(t)$ represents the risk-free value of the option, whereas $V_1(t)$ represents the risky value of the option. This composition of two terms also needs to be taken into account when determining hedging position $\eta_1(t)$: do we hedge only $V(t)$ or also $\text{CVA}(t)$?

First, the market $(S(t), V_i(t) \text{ and } H_i(t))$ is simulated using a model (e.g., Black-Scholes or Merton jump-diffusion). While valuing the portfolio, these numbers are assumed to be exogenous, meaning there is no longer a model dependence. The model used to compute the hedging quantities and perform the P&L explain needs to be calibrated to the market. When this model is the same as the model used to simulate the market, the calibration is trivial.

We use two strategies, Π^{NoCCR} and Π^{CCR} , to assess the effect of CCR. The former corresponds to the portfolio without simulation of defaults, while the latter includes CCR by simulating default times. In all cases, the hedges are rebalanced daily and assumed to be free of CCR. The simulated *default times* $\tau = t_d$ are drawn from the same distribution that drives the credit curve. So, the simulated default times are the first jumps of $X_{\mathcal{P}}(t)$. In the experiments, we assume a *risk-free closeout*, where we give back V_1 to the defaulted counterparty, and in return receive $R \cdot V(\tau)$ in case this value is positive. We assume stock $S(t)$ to be independent of any default events of the counterparty. At default, we re-enter the same deal with another counterparty which is assumed to be credit-risk free, for example a clearing house. This approach is in line with considering the CVA as the cost of hedging counterparty credit risk, regardless of a counterparty default. If the CVA is hedged, this hedge position is closed at default.

4.3. Black-Scholes dynamics

So far we have not assumed any model for S and $V_1(t)$, only a choice of credit curve and simulation of defaults was made. The next step is to assume a model for S and $V_1(t)$. Our first choice is the Black-Scholes model that allows for analytical option prices and derivatives, in a deterministic interest rate setting. Recall the Black-Scholes SDE under real-world measure \mathbb{P} :

$$dS(t) = \mu S(t) dt + \sigma S(t) dW^{\mathbb{P}}(t). \quad (4.5)$$

For the simulation of the market scenarios, the SDE (4.5) is discretized using an Euler scheme. The risk introduced by the underlying stock is eliminated when choosing the Black-Scholes delta hedging quantity:

$$\eta_1(t) = -\frac{\partial V_1(t)}{\partial S}. \quad (4.6)$$

In the risk-free case where $V_1(t) = V(t)$, hedging quantity (4.6) holds directly. On the other hand, in the risky case $V_1(t) = V(t) - \text{CVA}(t)$, where CVA is hedged, we can write the following using result (4.2):

$$\eta_1(t) = -\frac{\partial V(t)}{\partial S} (1 - (1 - R) \text{PD}(t, t_K)). \quad (4.7)$$

The \mathbb{P} dynamics given in Equation (4.5) are used for the simulation of a synthetic market. On the other hand, for pricing options and calculating risks as in Equations (4.6) and (4.7) we need \mathbb{Q} dynamics. To obtain these, in Equation (4.5) we choose $\mu = r$ and use a risk-neutral Brownian motion.

The simulation is illustrated by a series of schematic drawings that indicate the flow of cash and instruments, see Appendix C. There, we first consider the case without CCR to get a basic understanding of the mechanics of the trading strategy from the perspective of a bank. Then, CCR is introduced, and the bank's trading desk and xVA desk are represented as a single entity, referred to as the trading desk. Finally, we remove this assumption by examining the internal exchange of cash-flows and products between the desks.

4.4. Merton jump-diffusion dynamics

Jump-diffusion models aim to overcome the Black-Scholes assumption of constant implied volatility, by introducing independently distributed jumps in the dynamics. They can generically be defined as [7]:

$$dX(t) = \mu dt + \sigma dW^{\mathbb{P}}(t) + J(t)dX_J^{\mathbb{P}}(t), \quad S(t) = e^{X(t)}. \quad (4.8)$$

The *jumps* J arrive according to *Poisson process* $X_J^{\mathbb{P}}(t)$ that is assumed to be independent of the Brownian process $W^{\mathbb{P}}(t)$. Typical choices of jump size J distributions are a double exponential distribution as introduced by Kou [26] or normally distributed jumps as introduced by Merton [23]. We choose to work with the latter. Jump magnitudes in this model follow distribution $J \sim \mathcal{N}(\mu_J, \sigma_J^2)$.

For the simulation of a synthetic market we use an Euler discretization of the \mathbb{P} dynamics from Equation (4.8). On the other hand, for pricing options and calculating risks we need \mathbb{Q} dynamics. To obtain these, in Equation (4.8) we should choose the drift as follows ¹⁰:

$$\mu = r - \xi_J \mathbb{E}[e^J - 1] - \frac{1}{2}\sigma^2 = r - \xi_J \left(e^{\mu_J + \frac{1}{2}\sigma_J^2} - 1 \right) - \frac{1}{2}\sigma^2.$$

Furthermore, we use a risk-neutral Brownian motion and jump process in the \mathbb{Q} dynamics, which are again assumed to be independent. For European option prices under the Merton jump-diffusion model an analytic expression exists, see Appendix A.1.

After simulating the market $S(t) = e^{X(t)}$ with the Merton model, we compute the Merton option price using Equation (A.1). Here we do not make an assumption on $V_1(t)$ being a risk-free or risky option value (without CVA versus with CVA). Distinguishing between the two cases can be done in a similar fashion as discussed in Section 4.3. For setting up the hedging position $\eta_1(t)$, we consider the following three approaches.

The first approach is applicable to the situation where the institution's pricing model is misaligned with the market. In our setup, this is represented by using a Black-Scholes delta hedge as in Section 4.3, even though the market does not follow these dynamics. This is done by extracting the Black-Scholes implied volatility from the Merton option prices observed in the market, and setting up a Black-Scholes delta hedge using the underlying stock. We confirm the results by Naik and Lee [30] that this hedging strategy is not suitable for the case of an underlying asset driven by both diffusion and jump risk.

The second approach represents the case in which one's pricing model is perfectly aligned with the market. In this context this means that the Merton delta, as in Equation (A.5), can be used to compute the hedging quantity. Equations (4.6) and (4.7) still hold in this case, given that the Black-Scholes deltas are replaced by Merton deltas.

Up to this point, no attempt has been made to hedge the jump risk introduced by the Merton model. The option pricing formula (A.1) contains an infinite sum of scaled Black-Scholes option prices, which is a direct result of the jump size following a continuous distribution. Thus, in an attempt to hedge the jump risk introduced by the model, one would theoretically need infinitely many options, which is practically infeasible. Hedging the jump risk has been addressed by adding a number of options to the hedging portfolio [6, 16]. This significantly reduces the variance of the portfolio. In particular, a local minimal variance hedging strategy was examined, combined with a delta position in the underlying stock. In this paper, we use the analytical jump parameter sensitivities from Appendix A.1 to determine the hedging positions that aim to eliminate the underlying jump risk.

¹⁰In this case we can use the known result that for $A \sim \mathcal{N}(\mu, \sigma^2)$ we know $\mathbb{E}[e^A] = e^{\mu + \frac{1}{2}\sigma^2}$.

The third approach includes the hedging of jump risk by adding single option to the set of hedging instruments, i.e., we have $H_1(t) = S(t)$ and $H_2(t)$, which is a European option different from option $V_1(t)$ we aim to hedge. Option $H_2(t)$ is a risk-free option, such that no additional xVAs are introduced. To summarize, we have:

$$\Pi(t) = V_1(t) + \eta_1(t)S(t) + \eta_2(t)H_2(t).$$

We choose stock position $\eta_1(t)$ such that the portfolio is delta-neutral, i.e., such that $\frac{\partial \Pi(t)}{\partial S} = 0$:

$$\eta_1(t) = -\frac{\partial V_1(t)}{\partial S} - \eta_2(t) \frac{\partial H_2(t)}{\partial S}.$$

This leaves the question of how to choose $\eta_2(t)$. We use analytical jump parameter sensitivities to determine the remaining hedging position. As the strategy contains one hedging option, we must choose one of the jump parameters that we consider most important. All jump parameters have a level effect, μ_J also affects the skew, and σ_J also affects the curvature, see Appendix A.2. The level effect from ξ_J is more significant than that for μ_J and σ_J . Hence, we choose ξ_J to set up the hedge. So, for $\eta_2(t)$ we have:

$$\eta_2(t) = -\frac{\partial V_1(t)}{\partial \xi_J} \left[\frac{\partial H_2(t)}{\partial \xi_J} \right]^{-1}. \quad (4.9)$$

The partial derivatives w.r.t. ξ_J are computed analytically using the result in Equation (A.4). The hedging strategy as presented here is equivalent to first taking a position in the stock $\eta_1(t)$ to hedge the trading instrument (so Equation 4.6 but with the Merton delta), then taking position (4.9) to hedge the jump risk, and then updating $\eta_1(t)$ to account for the additional delta risk generated by this position in the hedging option.

5. Numerical results

We implement the market simulation, as introduced in Section 4, in a Monte Carlo setting. In our experiments, we simulate the synthetic market and do all pricing under the \mathbb{Q} dynamics. The algorithm used to obtain the numerical results is summarized below (Algorithm 1).

All results are obtained with the following parameters: $t_0 = 0$, $T = 1$, $S(t_0) = 100$, $r = 0.1$, $\sigma = 0.2$, $K = 0.95$, $\xi_P = 0.2$, and $R = 0.5$. For the Merton jump-diffusion parameters we choose $\sigma_J = 0.1$, $\mu_J = -0.125$, and $\xi_J = 0.1$. We use $L = 10^5$ Monte Carlo paths and 200 time steps per year to create the set of monitoring dates. The results are displayed using a number of 100 shares for the option, such that the controlled notional by the option is 10^4 . As a result, the vertical axes of the plots can be interpreted as errors in bps. Furthermore, in the results the bank is represented as a single entity, meaning that the trading desk and xVA desk do not have separate trading strategies and wealth accounts. This split in the results can easily be made using the schematic drawings in Appendix C, but here we do not do this for sake of brevity.

5.1. Hedging CVA in a Black-Scholes setting

The first numerical results correspond to the Black-Scholes hedging setting as discussed in Section 4.3. In this section, the Black-Scholes model is used for market simulation, computing hedging quantities, and P&L explain.

5.1.1. CVA as a cash amount

In Figure 1a we confirm a guaranteed loss at maturity if the counterparty could default, but no CVA is charged. This is done by examining the impact of simulated defaults on the portfolio, where a guaranteed loss is represented by $\mathbb{E}_{t_0}[\Pi^{CCR}(t_K) + w^{CCR}(t_K)] < 0$. For Π^{NoCCR} we have the desired result, namely $\mathbb{E}_{t_0}[\Pi^{NoCCR}(t_K) + w^{NoCCR}(t_K)] \approx 0$, with some residual noise coming from the Monte Carlo simulation. The terminal wealth distribution in Figure 1b can be interpreted as a bimodal distribution. The large peak corresponds to the paths without default, whereas the low and wide peak on the left corresponds to the losses encountered as a result of defaults.

```

Input: Trading strategies  $\Pi^{\text{NoCCR}}$  and  $\Pi^{\text{CCR}}$ , risk factors  $\gamma$ , number of simulation paths  $L$  and dates  $K$ 
Output: Numerical results of the CVA hedging exercise
1 Initialize two portfolios  $\Pi^{\text{NoCCR}}$  and  $\Pi^{\text{CCR}}$ 
2 Initialize simulation grid of risk factors  $\gamma$ 
3 for  $l \leftarrow 1$  to  $L$  do
4   for  $k \leftarrow 1$  to  $K$  do
5     Simulate all risk factors  $\gamma(t_k)$  for path  $l$ 
6     Re-value  $\Pi^{\text{NoCCR}}(t_k)$  and  $\Pi^{\text{CCR}}(t_k)$  for path  $l$ 
7     for  $i \leftarrow 1$  to  $N$  do
8       | Re-value  $V_i(t_{k-1}, t_k)$  for path  $l$  to be used later in the P&L calculations
9     end for
10    for  $j \leftarrow 1$  to  $M$  do
11      | Re-value  $H_j(t_{k-1}, t_k)$  for path  $l$  to be used later in the P&L calculations
12    end for
13  end for
14  Simulate default time  $\tau_l$ 
15  Perform closeout at default time  $\tau_l$  for  $\Pi^{\text{CCR}}$ 
16  for  $k \leftarrow 1$  to  $K$  do
17    | Compute the relevant P&L quantities at time  $t_k$ , prepare P&LE for path  $l$ 
18    | Compute wealth  $w^{\text{NoCCR}}$  and  $w^{\text{CCR}}$  for path  $l$ 
19  end for
20 end for
21 Compute required output metrics and visualize results

```

Algorithm 1: CVA hedging algorithm

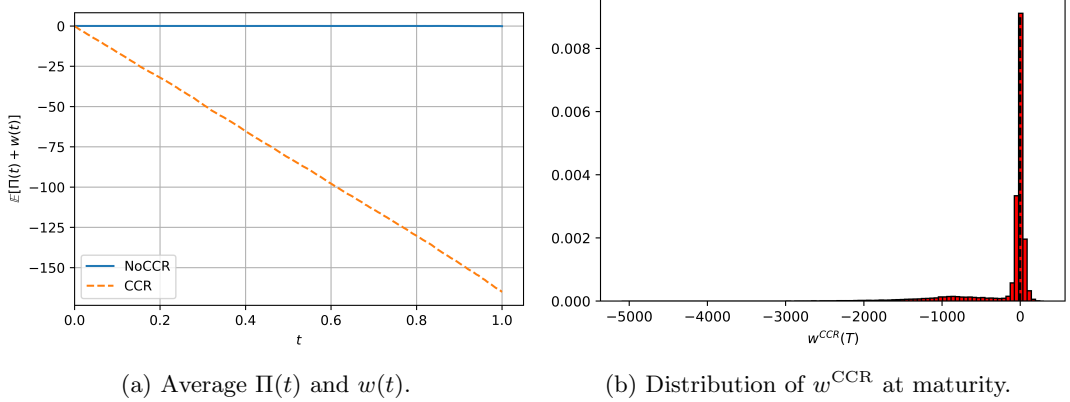


Figure 1: CVA not included in the portfolio.

Intuitively, $\mathbb{E}_{t_0}[\Pi^{\text{CCR}}(t_K) + w^{\text{CCR}}(t_K)] \approx \text{CVA}(t_0) \frac{B(t_K)}{B(t_0)}$ should hold. Hence, we add the CVA charge at inception as a cash amount to the wealth account, meaning that we perform a linear shift in initial wealth. This should result in $\mathbb{E}_{t_0}[\Pi^{\text{CCR}}(t_K) + w^{\text{CCR}}(t_K)] \approx 0$, which is indeed the case, see Figure 2a. So, the CVA charge proves to be a fair compensation of the credit riskiness of the counterparty. Furthermore, we see in Figure 2b that the distribution of $w^{\text{CCR}}(t_K)$ gets shifted to the right due to the CVA charge added at inception. The shift is precisely the required amount such that the mean of the distribution is around zero.

We see that charging the CVA at inception to the client and putting it on the wealth account overcomes the issue of a guaranteed loss. However, treating the CVA charge as a cash number with no dependencies on underlying market variables is not useful in practice and naive. In practice, the CVA is charged to the client at trade inception. As time passes, changes in the market result in a change in CVA.

5.1.2. CVA driven by market risk

Next, we consider the CVA to be driven by market risk, but we decide not to hedge this risk. This means we use the hedging quantity from Equation (4.6) with the risk-free Black-Scholes delta, even though we have $V_1(t) = V(t) - \text{CVA}(t)$. From now on, we refer to the case

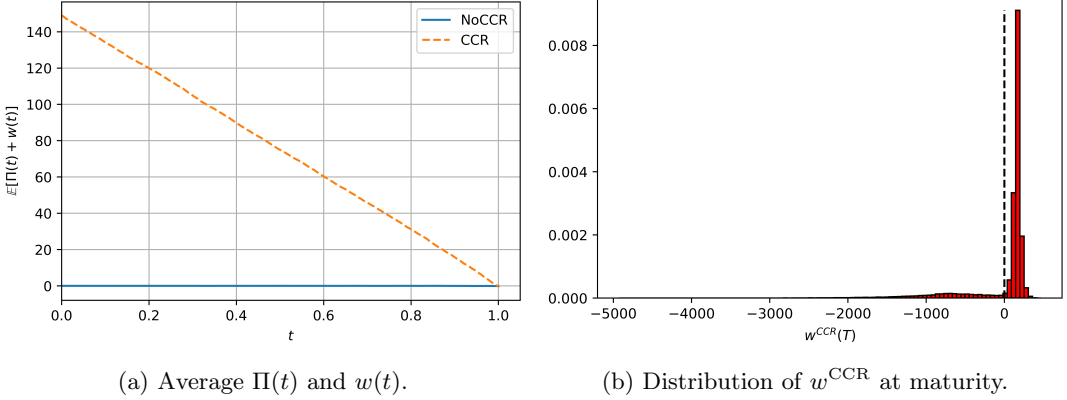


Figure 2: CVA included in the portfolio as a cash amount.

of Black-Scholes paths and delta as the pure Black-Scholes case.

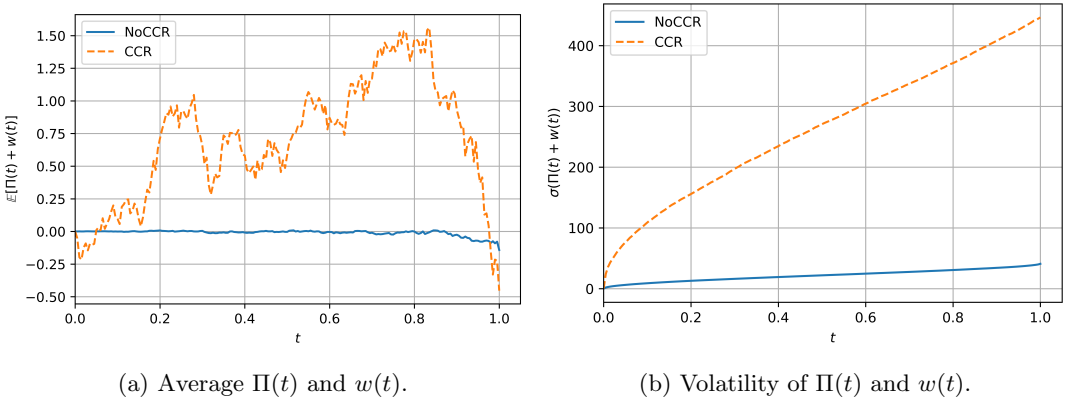


Figure 3: Comparison of Π^{NoCCR} and Π^{CCR} using a Black-Scholes market and valuation model. CVA is not hedged.

Figure 3a represents the case in which CVA was added to the portfolio but not hedged. We see that the expected terminal wealth condition $\mathbb{E}_{t_0}[\Pi(t_K) + w(t_K)] = 0$ is satisfied. In Figure 3b, we see that the variability of $\Pi(t) + w(t)$ for Π^{CCR} is much higher compared to that of Π^{NoCCR} . This is expected as a result of the additional source of randomness introduced by the simulated defaults in Π^{CCR} . $\Pi(t) + w(t)$ must always be examined first when assessing the performance of the portfolio, but it does not guarantee optimal performance.

Therefore, consider Figures 4a and 4b, where we plot the mean and volatility of $\text{P\&L}_P(t)$. One can clearly see that even though the mean P\&L_P for Π^{CCR} is slightly lower compared to Π^{NoCCR} , the volatility is significantly higher over the majority of the lifetime of the option. Thus, this hedging strategy is incomplete. The two lines in Figure 4b overlap close to maturity, because the binarity of the payoff takes over. Furthermore, most of the simulated defaults have occurred by this time. Because after a default the same deal is entered with a credit risk free counterparty, the two portfolios eventually exhibit similar behaviour. From Figures 4c and 4d we see that a significant portion of the $\text{P\&L}_P(t)$ can be explained using the underlying stock.¹¹ We see that the potential defaults through the lifetime of the option contribute to a significant initial difference in P\&L_U . This difference diminishes over time, as fewer defaults are expected to occur before the maturity of the option. As the strong increase in variance is not promising at a first glance, in Section 5.1.3 a thorough analysis of this behaviour can be found. All in all, the results indicate that CVA needs to be hedged to eliminate the majority of the underlying risk in the portfolio.

¹¹In case a delta hedge was employed to hedge first order risks, this term was ignored in the P&L explain process to avoid taking the delta effect into account twice.

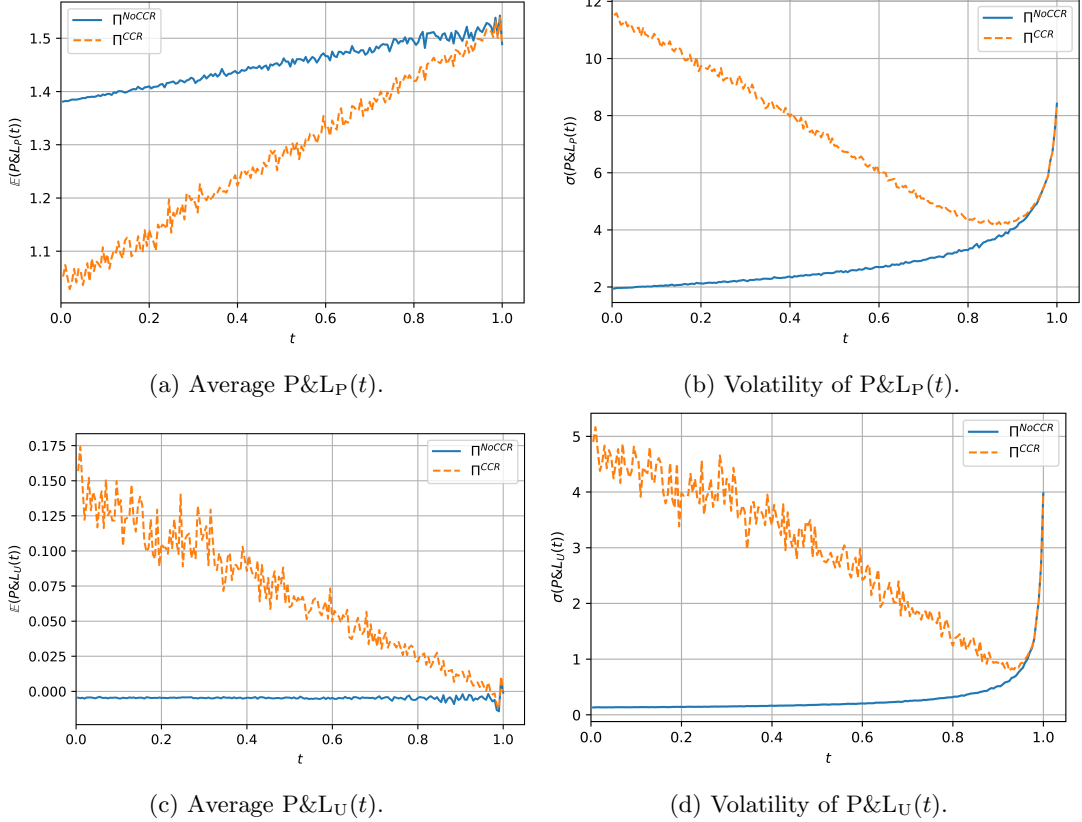


Figure 4: Comparison of Π^{NoCCR} and Π^{CCR} using a Black-Scholes market and valuation model. CVA is not hedged.

Looking at Figure 4a, one might question why the average $\text{P\&L}_P(t_0)$ for Π^{NoCCR} is not equal to zero, as this would mean that a Black-Scholes delta-hedge is unable to hedge all the risk of the option. Figure 5a shows that this number converges to zero if $dt \rightarrow 0$, so our observations are merely the result of the discretization. The volatility of $\text{P\&L}_P(t_0)$ for Π^{NoCCR} also converges to zero if the number of time-steps in the discretization is increased.

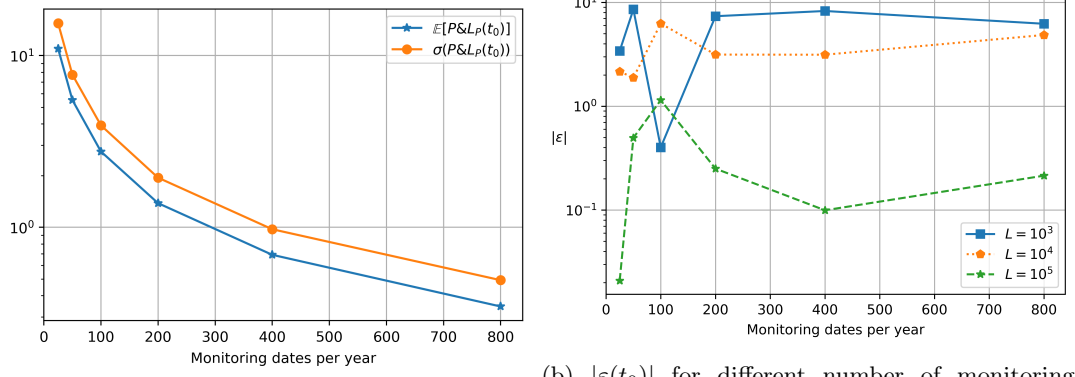
We also confirm that the CVA as charged initially covers the otherwise experienced loss at default. We do this by confirming that the following error measure is approximately zero:

$$\begin{aligned} \varepsilon(t_0) &= \mathbb{E}_{t_0} \left[\mathbb{1}_{\{\tau \leq t_K\}} \left[\frac{B(t_0)}{B(\tau)} (RV(\tau) - V(\tau)) + \text{CVA}(t_0) \right] + \mathbb{1}_{\{\tau > t_K\}} \text{CVA}(t_0) \right] \\ &\approx \frac{1}{L} \sum_{l=1}^L \mathbb{1}_{\{\tau_l \leq t_K\}} \left[\frac{B(t_0)}{B(\tau_l)} (RV(\tau_l) - V(\tau_l)) + \text{CVA}(t_0) \right] + \mathbb{1}_{\{\tau_l > t_K\}} \text{CVA}(t_0), \end{aligned} \quad (5.1)$$

where L denotes the number of Monte Carlo paths used in the simulation. We analyze the behaviour of this error measure by changing the number of Monte Carlo paths and number of time-steps used in the simulation. From Figure 5b we see that for a given number of monitoring dates per year, increasing the number of paths results in $|\varepsilon(t_0)| \rightarrow 0$. Here we clearly see that using $L = 10^3$ provided unstable results, but we do observe converging behaviour when increasing L . As defaults occur infrequently, the number of paths must be large to properly approximate the numerical expectation from Equation (5.1). Furthermore, the choice of 200 monitoring dates per year appears to be a very fine tradeoff between speed and accuracy.

5.1.3. Variance analysis

In Figure 4b we see an exploding behaviour in the volatility of P\&L_P as $t \rightarrow T$, for both Π^{NoCCR} and Π^{CCR} , which we want to understand. Therefore, we explain the distribution features we observe by looking at the P\&L_P mean and variance for Π^{NoCCR} . Thus, we examine



(a) Π^{NoCCR} results of $P\&L_P(t_0)$ average and dates, per different number of Monte Carlo paths volatility for different number of monitoring dates. L .
(b) $|\epsilon(t_0)|$ for different number of monitoring

Figure 5

$P\&L_P$ for the portfolio in Equation (4.3), with the Black-Scholes delta hedging quantity as in Equation (4.6). $P\&L_P$ from Equation (3.10) can be rewritten as follows:

$$\begin{aligned} P\&L_P(t_k) &= \Pi(t_{k-1}, S(t_k)) - \Pi(t_{k-1}, S(t_{k-1})) \\ &= [V_1(t_{k-1}, S(t_k)) - V_1(t_{k-1}, S(t_{k-1}))] + \eta_1(t_{k-1}) [S(t_k) - S(t_{k-1})]. \end{aligned} \quad (5.2)$$

Dividing both sides of Equation (5.2) by $dS = S(t_k) - S(t_{k-1})$, and using the definition of a forward finite difference approximation yields:

$$\begin{aligned} \frac{P\&L_P(t_k)}{S(t_k) - S(t_{k-1})} &= \frac{V_1(t_{k-1}, S(t_k)) - V_1(t_{k-1}, S(t_{k-1}))}{S(t_k) - S(t_{k-1})} - \frac{\partial V_1(t_{k-1})}{\partial S} \\ &= \frac{dS}{2} \frac{\partial^2 V_1(t_{k-1}, S(t_{k-1}))}{\partial S^2} + \mathcal{O}((dS)^2), \end{aligned} \quad (5.3)$$

$$\Rightarrow P\&L_P(t_k) = \frac{(dS)^2}{2} \frac{\partial^2 V_1(t_{k-1}, S(t_{k-1}))}{\partial S^2} + \mathcal{O}((dS)^3). \quad (5.4)$$

Equation (5.4) shows that two types of errors drive $P\&L_P$. First, there is the truncation error of the forward finite differences which are used in Equation (5.3). Furthermore, there is a discretization error that disappears if $dS \rightarrow 0$, which will happen if $dt = t_k - t_{k-1} \rightarrow 0$.

In Equation (5.4), we recognize the second partial derivative as the option gamma, which under the Black-Scholes model is given by the following analytic expression:

$$\begin{aligned} \frac{\partial^2 V_1(t, S)}{\partial S^2} &= K e^{-r(T-t)} \frac{\phi(d_2(t, S))}{S^2 \sigma \sqrt{T-t}}, \\ d_2(t, S) &= \frac{\ln \frac{S}{K} + (r - \frac{1}{2} \sigma^2) [T - t]}{\sigma \sqrt{T-t}}. \end{aligned} \quad (5.5)$$

Define $X \sim \mathcal{N}(\mu_X, \sigma_X^2)$ such that $S(t_k) \stackrel{d}{=} S(t_{k-1}) e^X$, see Appendix B for further details. Using this and the Black-Scholes gamma (5.5), we rewrite Equation (5.4) as follows:

$$\begin{aligned} P\&L_P(t_k) &= \frac{(dS)^2}{2} K e^{-r\tau} \frac{\phi(d_2(t_{k-1}, S(t_{k-1})))}{S^2(t_{k-1}) \sigma \sqrt{\tau}} + \mathcal{O}((dS)^3) \\ &= \frac{S^2(t_{k-1}) [\ln \frac{S}{K} + (r - \frac{1}{2} \sigma^2) \tau]^2}{2} K e^{-r\tau} \frac{\phi(d_2(t_{k-1}, S(t_{k-1})))}{S^2(t_{k-1}) \sigma \sqrt{\tau}} + \mathcal{O}((dS)^3) \\ &= \frac{K e^{-r\tau}}{2 \sigma \sqrt{\tau}} [\ln \frac{S}{K} + (r - \frac{1}{2} \sigma^2) \tau]^2 \phi(d_2) + \mathcal{O}((dS)^3), \end{aligned} \quad (5.6)$$

where $\tau := T - t_{k-1}$ and for ease of notation we write $d_2 = d_2(t_{k-1}, S(t_{k-1}))$.

Define $d_2 \sim \mathcal{N}(\mu_{d_2}, \sigma_{d_2}^2)$, see Appendix B. Then, using definitions (B.13) and (B.14) for respectively $f(\mu_X, \sigma_X)$ and $g(\mu_X, \sigma_X)$, we obtain this expression of the variance of P&L_P:

$$\text{Var}_{t_0}(\text{P&L}_P(t_k)) \approx \frac{K^2 e^{-2r\tau}}{8\pi\sigma^2\tau} \left[f(\mu_X, \sigma_X) \cdot \frac{e^{-\frac{\mu_{d_2}^2}{1+2\sigma_{d_2}^2}}}{\sqrt{1+2\sigma_{d_2}^2}} - g(\mu_X, \sigma_X) \cdot \frac{e^{-\frac{\mu_{d_2}^2}{1+\sigma_{d_2}^2}}}{1+\sigma_{d_2}^2} \right]. \quad (5.7)$$

See Appendix B for a full derivation of this result.

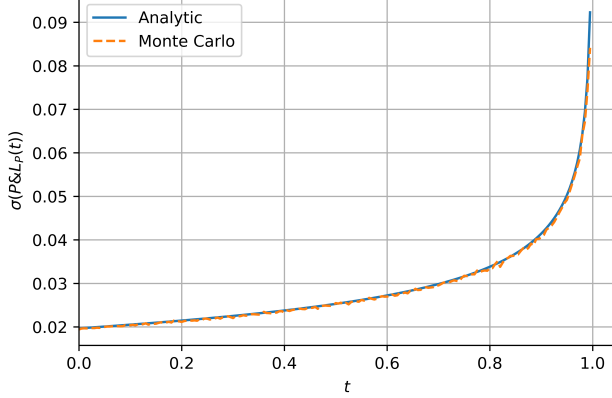


Figure 6: Numerical confirmation that the analytical variance for Π^{NoCCR} from Equation (5.7) is in line with the Monte Carlo simulation.

From Figure 6 we see that the analytical result from Equation (5.7) and volatility from the Monte Carlo simulation are in line. The strong increase of P&L_P volatility close to maturity can be understood from the perspective of P&L_P being driven by the option gamma, see Equation (5.4). It is known for the option delta to be instable near maturity, causing an increased gamma. This explains the increase in variance of P&L_P(t_k) as $t_k \rightarrow T$. Especially when the option is close to the ATM point, the gamma is large, causing a large gamma volatility.

Looking at Equation (5.7), the strong increase in volatility towards maturity can be explained by looking at the variance as a scaled difference between the factors $(\sqrt{1+2\sigma_{d_2}^2})^{-1}$ and $(1+\sigma_{d_2}^2)^{-1}$. The first term is non-linear, while the second is linear. Approaching maturity, the non-linearity of $(\sqrt{1+2\sigma_{d_2}^2})^{-1}$ increases, causing the increased variance.

5.1.4. Hedging CVA

In Section 5.1.2 we concluded that CVA needs to be hedged. Hence, we now hedge the market risk of the CVA using the underlying stock, summarized by the hedging quantity Equation (4.7). In terms of the zero average return, hedging the CVA yields the same results as not hedging. Comparing Figures 4a and 7a shows that the average P&L_P for Π^{CCR} is initially lower for the case where we do not hedge the CVA than when we do. However, this difference is not significant, especially not when taking the size of the volatility into consideration. In other words, the volatility appears to be a dominating factor in these results. Comparing Figures 4b and 7b shows a benefit of hedging the CVA, as this yields a significantly lower volatility in P&L_P. Hence, we again conclude that CVA must be hedged.

Regarding the P&L_U, the results from Figures 4c and 4d also hold for the situation with CVA hedge. This makes sense, as the CVA market risk is either hedged and then does not need to be explained, or it is not hedged but then could be explained. So, hedging CVA does not affect the result of how much P&L can be explained.

5.2. Hedging CVA in a Merton jump-diffusion setting

The numerical results in this section correspond to the Merton jump-diffusion hedging setting from Section 4.4. The market is simulated using the Merton jump-diffusion model. The hedging quantities and P&L_E are computed with various models, depending on the experiment.

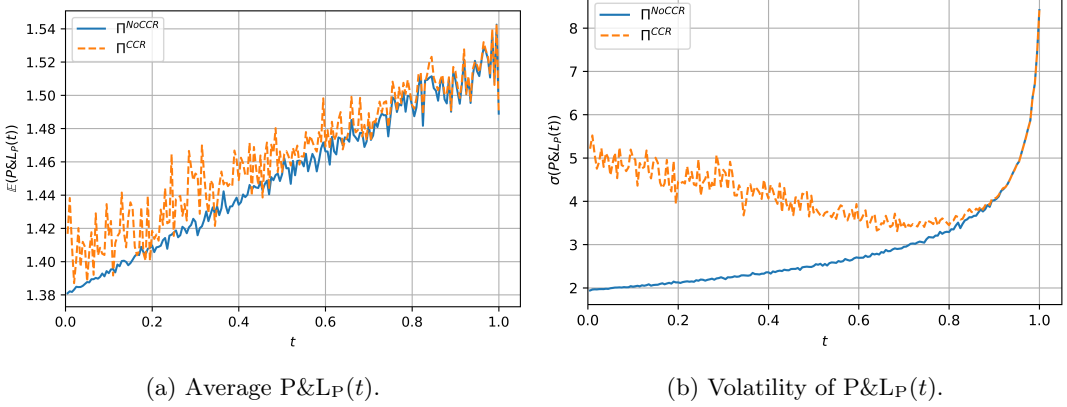


Figure 7: Comparison of Π^{NoCCR} and Π^{CCR} using a Black-Scholes market and valuation model. CVA is hedged using the underlying stock.

5.2.1. Black-Scholes delta hedge

Here, a Black-Scholes delta hedge takes place. Introducing jumps in the stock dynamics results in an extra source of randomness. In particular, $\Pi(t) + w(t)$ for Π^{NoCCR} shows roughly twice as much volatility through the option's lifetime. For Π^{CCR} , the simulated defaults appear to be dominating as there are no significant differences compared to the pure Black-Scholes case.

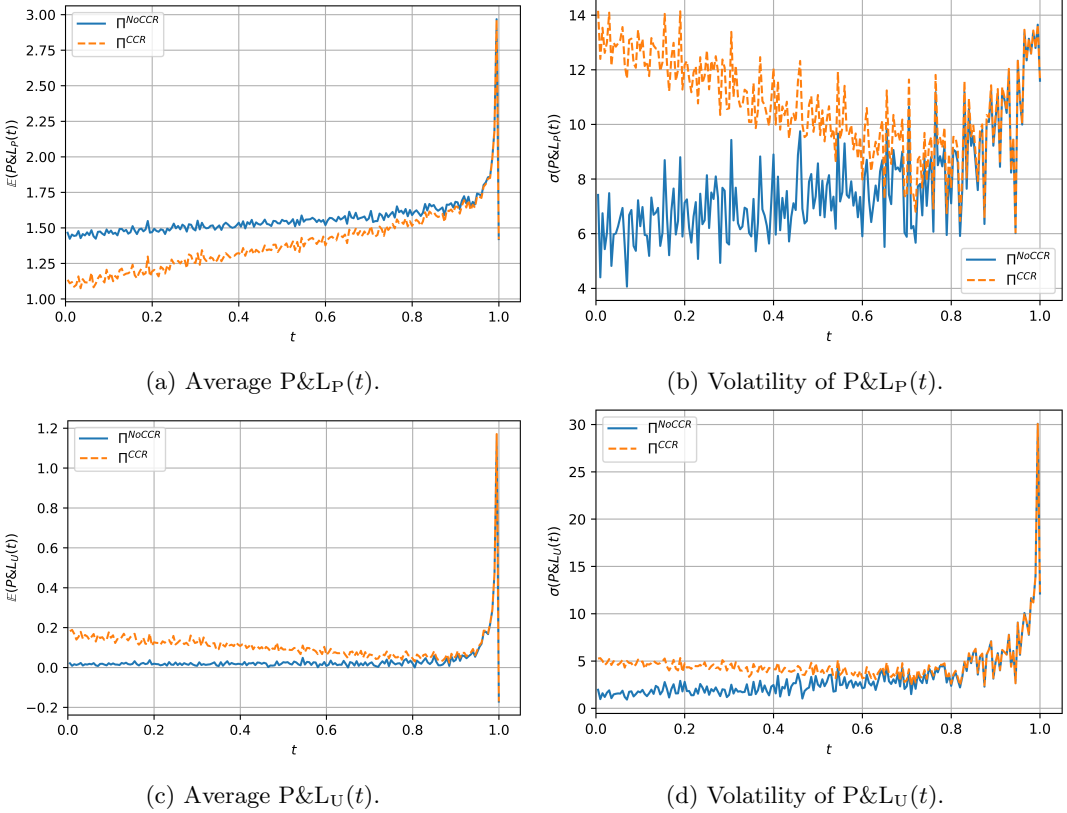


Figure 8: Comparison of Π^{NoCCR} and Π^{CCR} using a Merton market and a Black-Scholes valuation model. CVA is not hedged.

There are two observations when comparing the P&L mean in Figure 8a with the pure Black-Scholes results from Figure 4a. First, the level of the average is higher during the lifetime of the option. Second, a peak is observed close to maturity. This is the result of the Black-

Scholes delta's inability to cope with jumps just before maturity. In particular, a jump in the underlying stock for the paths where the option is close to the ATM point before maturity can result in a change of the option being in or out of the money. The volatility of $P\&L_P$ from Figure 8b is larger as well as significantly more variable over time when comparing with the pure Black-Scholes case (see Figure 4b), though the shape stays roughly the same. These results are in line with our expectations, as the Black-Scholes delta does not take into account the additional source of randomness from the stock jumps, so this risk is not hedged.

The average $P\&L_U$ in Figure 8c is slightly lower than the average $P\&L_P$. Yet the peak before maturity observed for $P\&L_P$ remains present, indicating that the hedging strategy in combination with the chosen model does not result in the desired results. Recall that this peak is not present in the pure Black-Scholes case (see Figure 4c). For the volatility of $P\&L_U$ in Figure 8d, the same reduction versus the $P\&L_P$ volatility is observed as in the pure Black-Scholes case (see Figure 4d). However, close to maturity the $P\&L_U$ volatility is even higher than the $P\&L_P$ volatility. This effect is the result of the gamma explain volatility just before maturity, which has significant peaks. The option gamma is the rate of change in the option delta w.r.t. changes in the underlying price. For the ATM cases, the delta is extremely sensitive to changes in the underlying asset. So, paths around the ATM level just before maturity cause this increase in $P\&L_U$ volatility. Furthermore, we observe significant movement in the volatility for the Merton case just before the maturity of the option. All this together is a clear indication that the jump effects are missing in the explain process.

The CVA hedge in this context has no effect on either $\Pi(t) + w(t)$ or $P\&L_U$, which is in line with our observations for the pure Black-Scholes case. For the $P\&L_P$ the same effect of the CVA hedge is observed as in the pure Black-Scholes case: the average $P\&L_P$ of Π^{CCR} overlaps significantly with that of Π^{NoCCR} after the introduction of the CVA hedge. Furthermore, the initial volatility in the Π^{CCR} is much lower in the case of a CVA hedge, and the volatilities overlap much earlier in the case of a CVA hedge.

Introducing jumps in the Merton dynamics indeed results in additional randomness when comparing with the pure Black-Scholes case, already before considering the CCR. For the case with CCR, the introduction of jumps in the stock seems to dominate the effect of the CCR in this case study. The CVA hedge has the same desired effects for both Black-Scholes and Merton paths, of course ignoring the additional randomness introduced by the Merton jumps. We can conclude that the Black-Scholes delta hedge in the case of a Merton market has its shortcomings. Therefore, as a next step, we compare these results with a Merton delta hedge.

5.2.2. Merton delta hedge

We now use the Merton delta hedge in a Merton market, and do not hedge the CVA. The only difference compared to the Black-Scholes delta hedge is in the average $P\&L_P$ and $P\&L_U$. For the $P\&L_P$, the peak close to maturity we observed in the case of a Black-Scholes delta hedge, see Figure 8a, has disappeared. For the $P\&L_U$, the big upward peak just before maturity, see Figure 8c, has disappeared too. A minor downward peak remains due to instability in the gamma explain. The Merton Greeks are not capable of mitigating these instabilities.

The effect of the CVA hedge is clearly visible in Figures 9a and 9b. After filtering out the effects of the Merton delta as described before, the CVA hedge yields the same conclusion as for the Black-Scholes delta hedge.

Overall, the impact of moving from the Black-Scholes delta hedge to the Merton delta hedge was significant, especially in the average $P\&L_P$. Yet some issues and undesired results remained, for example due to the instability of the gamma explain. Clearly we need another way to hedge away more of the jump risk associated with the Merton model.

5.2.3. Hedging the jump risk using an option

Therefore, we hedge the residual jump risk from the Merton model using an extra instrument in the hedging portfolio: one extra option. Typically, OTM options are chosen in the hedging portfolio as they are cheap. One of the difficulties resulting from Equation (4.9) is that $\frac{\partial H_2(t)}{\partial \xi_J}$ tends to zero close to maturity, due to the option being OTM. $\frac{\partial V_1(t)}{\partial \xi_J}$ may behave the same, however, it is likely that $\frac{\partial H_2(t)}{\partial \xi_J}$ will decay faster due to the option being deeper OTM. As a result, $\eta_2(t)$ in Equation (4.9) will increase drastically close to maturity of the option. For

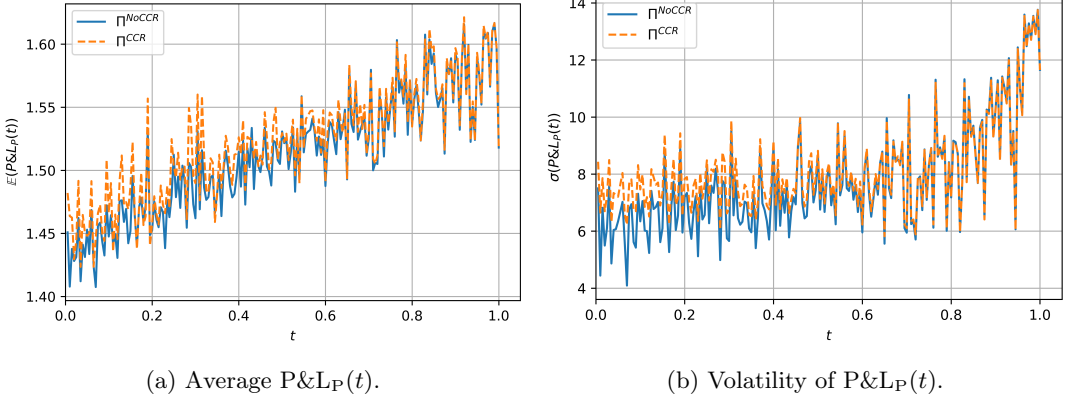


Figure 9: Comparison of Π^{NoCCR} and Π^{CCR} using a Merton market and valuation model. CVA is hedged using the underlying stock.

the hedging option we choose an OTM put with strike $K = 90$, maturity $T = 1$ and controlling the same number of shares as the original option we hedge. In case we hedge the CVA, this is done using both the underlying stock and same option we use to hedge the product itself.

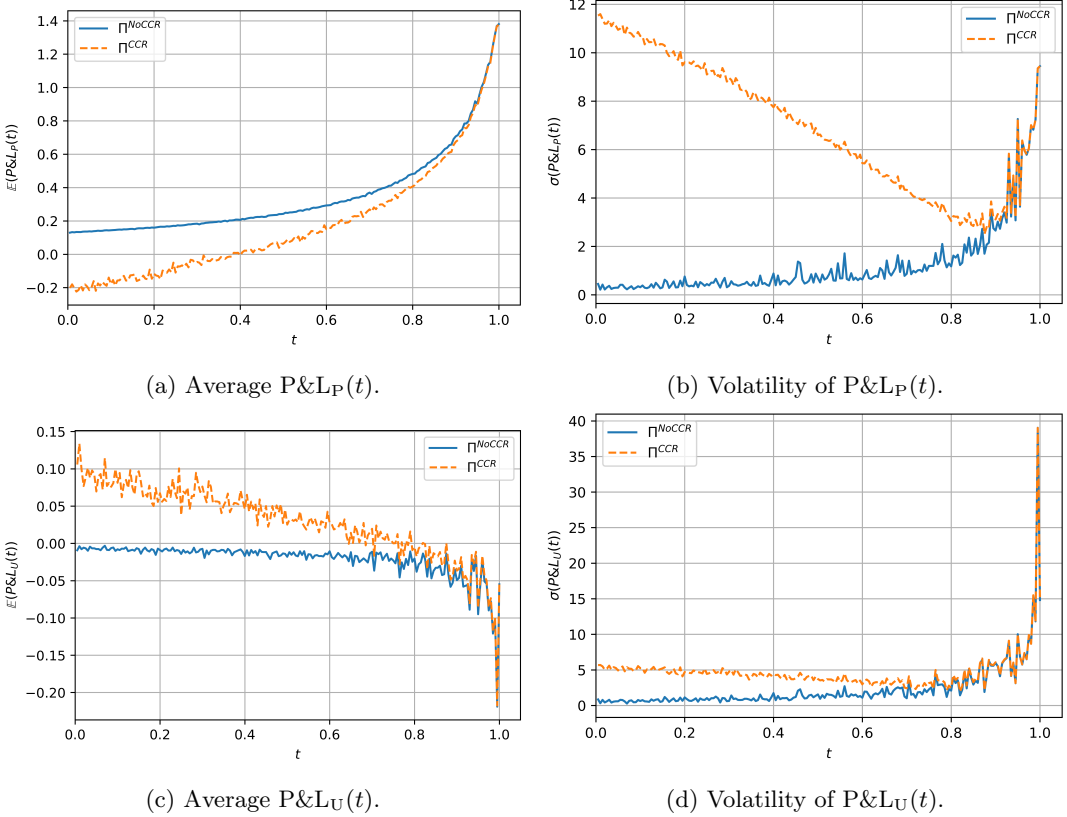


Figure 10: Comparison of Π^{NoCCR} and Π^{CCR} using a Merton market and valuation model. An additional option is added to the hedging portfolio. CVA is not hedged.

The effect of the single option hedge is clearly visible in the volatility of $\Pi(t) + w(t)$ for Π^{NoCCR} . Where for the Black-Scholes hedge we observe roughly twice as much as volatility through the lifetime of the option, we now observe results similar to the pure Black-Scholes case. So the single option hedge yields the desired effects. For Π^{CCR} , the CCR still dominates the jumps from the stock.

The mean $P\&L_P$ in Figure 10a exhibits a non-linear behaviour due to the additional optionality in the portfolio. The $P\&L_P$ volatility in Figure 10b is much lower compared to before, see Figure 8b. Again we observe the beneficial effects of the hedging option, as the results look more like the pure Black-Scholes case.

The average $P\&L_U$ in Figure 10c, compared to the Merton delta hedge, is comparable up to the same non-linear effect we also observe for the $P\&L_P$. Overall, the volatility in Figure 10d is comparable to the previous results in Figure 8d, except for a significantly higher peak just before maturity. This is the result of an exploding gamma explain volatility close to maturity.

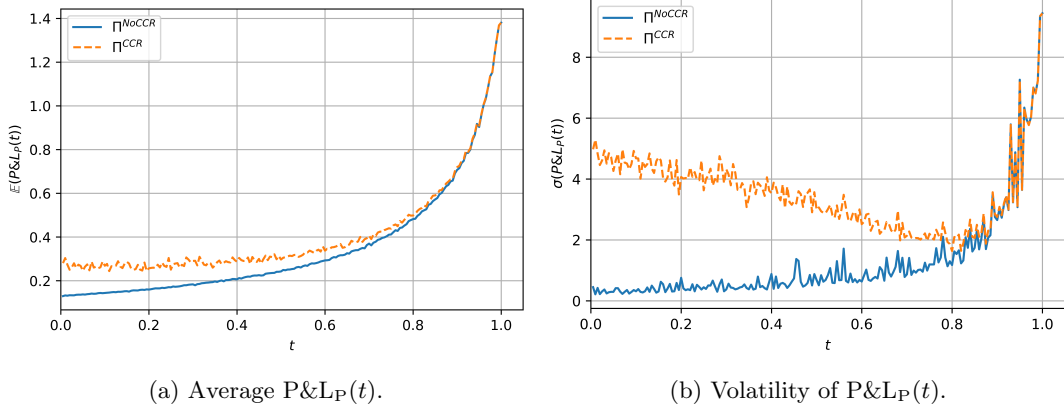


Figure 11: Comparison of Π^{NoCCR} and Π^{CCR} using a Merton market and valuation model. An additional option is added to the hedging portfolio. CVA is hedged using both the underlying stock and the additional option.

As before, the CVA hedge has no effect on $\Pi(t) + w(t)$ or $P\&L_U$, which is in line with our other observations so far. The effect of the CVA hedge on $P\&L_P$, see Figure 11, is similar to the effect in the pure Black-Scholes case. Especially the volatility, which is the dominating factor, is comparable to the pure Black-Scholes case (see Figure 7b). For the average we observe in Figure 11a that the Π^{CCR} is slightly above Π^{NoCCR} , which is also observed for the pure Black-Scholes case (see Figure 7a).

Adding the option to the hedging strategy has a clear effect of smaller $P\&L_P$ volatility. Increasing the number of options in the hedging strategy will likely increase the hedging performance, however, the effect of the first option is already significant [6, 16]. The increase in $P\&L_U$ volatility can be explained by the hedging option having a fixed strike. For some of the simulated paths, this hedge option may become significantly OTM, meaning the sensitivity to the jumps is close to zero. This results in a less effective hedge of the jump risk.

6. Conclusion

In conclusion, dynamic CVA hedging is now better understood, both in a Black-Scholes and a Merton jump-diffusion setting. Starting from a theoretical hedging framework, we have examined the mechanics of a trading strategy which included CVA pricing and hedging. We visualized cash-flows and exchanges of traded instruments of the portfolio. For a case study of a portfolio containing European options and the underlying stock, we used a Monte Carlo simulation to study hedging. Hedging performance was assessed by analyzing the trading strategy balance, including the corresponding wealth account. Furthermore, we studied the P&L behaviour of the strategy, as well as the performance of the P&L explain. In particular, analytic results helped us to explain and analyze P&L behaviour that was observed from the simulation.

First, in a Black-Scholes setting we showed that failing to charge CVA to a credit risky counterparty will result in an average guaranteed loss. We can see CVA as a fair compensation for this credit risk. Merely treating CVA as a cash amount turns out to be nave, as CVA is driven by market risk. In fact, failing to hedge the market risk component of CVA results in an unstable trading strategy, and thus implies the hedge in the portfolio is incomplete.

We have shown that CVA in a Black-Scholes context can satisfactorily be hedged using the underlying stock. For the P&L_P, we saw a significant increase in volatility as the option maturity approached. We showed that P&L_P is driven by the option gamma, which is known to become unstable close to maturity, especially for options that are close to the ATM point. Thus, the strong volatility increase is a direct consequence of the parameters chosen in our case study. CVA hedging significantly lowers the volatility P&L_P. Therefore, we conclude that hedging CVA is necessary for a stable trading strategy.

Next, we examined our case study portfolio when the underlying stock is driven by a Merton jump-diffusion process. A Black-Scholes delta hedge in this is incapable of dealing with the jump risk introduced by Merton's model. Hedging the CVA in this situation is still a must, though clearly something is missing from the strategy. Though using the Merton option deltas for the hedge is better than the Black-Scholes delta hedge, the effect is insufficient. Adding an option as a hedging instrument mitigates a significant part of the jump risk. Extending the hedging instruments with more options may result in an even more stable strategy.

All in all, the theoretical hedging framework in which dynamic CVA hedging has been studied allows one to consider a broad selection of trading strategies, but above all different and more xVAs. Understanding the mechanics of CVA hedging is a crucial first step for future research on xVA hedging.

Acknowledgements

This work has been financially supported by Rabobank.

References

- [1] A. Green. *XVA: Credit, Funding and Capital Valuation Adjustments*. Wiley Finance, first edition, November 2015. ISBN 978-1-118-55678-8.
- [2] A. Pallavicini, D. Perini, D. Brigo. Funding Valuation Adjustment: a consistent framework including CVA, DVA, collateral, netting rules and re-hypothecation. *arXiv Electronic Journal*, December 2011.
- [3] A. Pallavicini, D. Perini, D. Brigo. Funding, Collateral and Hedging: uncovering the mechanics and subtleties of funding valuation adjustments. *arXiv Electronic Journal*, December 2012.
- [4] B. Dupire. Pricing with a Smile. *Risk*, 7:18–20, January 1994.
- [5] C. Burgard, M. Kjaer. Partial differential equation representations of derivatives with bilateral counterparty risk and funding costs. *The Journal of Credit Risk*, 7(3):1–19, September 2011.
- [6] C. He, J.S. Kennedy, T. Coleman, P.A. Forsyth, Y. Li, K. Vetzal. Calibration and Hedging under Jump Diffusion. *Review of Derivatives Research*, 9(1):1–35, January 2006.
- [7] C.W. Oosterlee, L.A. Grzelak. *Mathematical Modeling and Computation in Finance*. World Scientific, first edition, November 2019. ISBN 978-1-78634-794-7.
- [8] D. Brigo, A. Capponi. Bilateral Counterparty Risk Valuation with Stochastic Dynamical Models and Application to Credit Default Swaps. *arXiv Electronic Journal*, November 2009.
- [9] D. Brigo, A. Pallavicini, V. Papatheodorou. Arbitrage-free valuation of bilateral counterparty risk for interest-rate products: impact of volatilities and correlations. *Mathematical Finance*, 14(6):773–802, July 2011.
- [10] D. Brigo, M. Masetti. Risk Neutral Pricing of Counterparty Risk. November 2005.
- [11] D. Duffie. *Dynamic Asset Pricing Theory*. Princeton University Press, third edition, November 2001. ISBN 978-0-691-09022-1.
- [12] E. Derman, I. Kani. Stochastic Implied Trees: Arbitrage Pricing with Stochastic Term and Strike Structure of Volatility. *International Journal of Theoretical and Applied Finance*, 1:61–110, 1998.
- [13] I. Arregui, B. Salvador, C. Vázquez. PDE models and numerical methods for total value adjustment in European and American options with counterparty risk. *Applied Mathematics and Computation*, 308:31–53, September 2017.
- [14] J. Gregory. Being two-faced over counterparty credit risk. *Risk*, February 2009.
- [15] J. Gregory. *The xVA Challenge - Counterparty Credit Risk, Funding, Collateral and Capital*. Wiley Finance, third edition, September 2015. ISBN 978-1-119-10941-9.
- [16] J.S. Kennedy, P.A. Forsyth, K. Vetzal. Dynamic Hedging Under Jump Diffusion with Transaction Costs. *Operations Research*, 57(3):541–559, May 2009.
- [17] L. Boen. European rainbow option values under the two-asset Merton jump-diffusion model. *Journal of Computational and Applied Mathematics*, 364, January 2020.
- [18] L.B.G. Andersen, V.V. Piterbarg. *Interest Rate Modeling - Volume III: Products and Risk Management*. Atlantic Financial Press, first edition, 2010. ISBN 978-0-98442-212-8.
- [19] M. Pythkin, S. Zhu. A Guide to Modeling Counterparty Credit Risk. *GARP Risk Review*, July/August(37):16–22, July 2007.
- [20] P. Henry-Labordere. Cutting CVA's complexity. *Risk*, 25:67–73, July 2012.
- [21] P. Henry-Labordere, X. Tan, N. Touzi. A numerical algorithm for a class of BSDEs via the branching process. *Stochastic Processes and their Applications*, 124(2):1112–1140, February 2014.

- [22] P.S. Hagan, D. Kumar, A.S. Lesniewski, D.E. Woodward. Managing Smile Risk. *Wilmott Magazine*, 3:84–108, September 2002.
- [23] R.C. Merton. Option pricing when the underlying stock returns are discontinuous. *Journal of Financial Economics*, 3(1-2):125144, January 1976.
- [24] S. Crepey. Bilateral counterparty risk under funding constraints - Part I: Pricing. *Mathematical Finance*, 25(1):1–22, January 2015.
- [25] S. Crepey. Bilateral counterparty risk under funding constraints - Part II: CVA. *Mathematical Finance*, 25(1):23–50, January 2015.
- [26] S.G. Kou. A Jump-Diffusion Model for Option Pricing. *Management Science*, 48(8):10861101, August 2002.
- [27] S.L. Heston. A Closed-Form Solution for Options with Stochastic Volatility with Applications to Bonds and Currency Options. *Review of Financial Studies*, 6(2):327–343, April 1993.
- [28] T.R. Bielecki, M. Rutkowski. Valuation and Hedging of Contracts with Funding Costs and Collateralization. *SIAM Journal on Financial Mathematics*, 6(1):594–655, July 2015.
- [29] U. Cherubini. Counterparty Risk in Derivatives and Collateral Policies The Replicating Portfolio Approach. July 2005.
- [30] V. Naik, M. Lee. General Equilibrium Pricing of Options on the Market Portfolio with Discontinuous Returns. *Review of Financial Studies*, 3(4):493–521, October 1990.

Appendix A. The Merton jump-diffusion model

Appendix A.1. Analytical European option prices and sensitivities

Here we re-iterate a result from [23, 7], namely the analytical expression for a European call option price on stock S , maturity T , and strike K , under the Merton jump-diffusion model:

$$\begin{aligned}
V(t) &= e^{-r(T-t)} \sum_{n \geq 0} \frac{[\xi_J(T-t)]^n e^{-\xi_J(T-t)}}{n!} \bar{V}(n), \\
\bar{V}(n) &= e^{\hat{\mu}_X(n) + \frac{1}{2}\hat{\sigma}_X^2(n)(T-t)} \Phi(d_1) - K \Phi(d_2), \\
\hat{\mu}_X(n) &= \log(S(t)) + \left[r - \xi_J \left(e^{\mu_J + \frac{1}{2}\sigma_J^2} - 1 \right) - \frac{1}{2}\sigma^2 \right] (T-t) + n\mu_J, \\
\hat{\sigma}_X(n) &= \sqrt{\sigma^2 + \frac{n\sigma_J^2}{T-t}}, \\
d_1 &= \frac{\log\left(\frac{S(t)}{K}\right) + \left[r - \xi_J \left(e^{\mu_J + \frac{1}{2}\sigma_J^2} - 1 \right) - \frac{1}{2}\sigma^2 + \hat{\sigma}_X^2(n) \right] (T-t) + n\mu_J}{\hat{\sigma}_X(n)\sqrt{T-t}}, \\
d_2 &= d_1 - \hat{\sigma}_X(n)\sqrt{T-t},
\end{aligned} \tag{A.1}$$

where r is the risk-free interest rate, σ is the stock volatility. Furthermore, μ_J , σ_J , and ξ_J are respectively the jump mean, volatility and intensity. In the case of a put option, one can simply apply the *put-call parity* to the call option price from Equation (A.1).

It can be shown that call price $V(t)$ from Equation (A.1) has the following analytical expressions of derivatives w.r.t. jump parameters μ_J , σ_J and ξ_J :

$$\frac{\partial V(t)}{\partial \mu_J} = e^{-r(T-t)} \sum_{n \geq 0} \frac{[\xi_J(T-t)]^n e^{-\xi_J(T-t)}}{n!} \left(n - \xi_J e^{\mu_J + \frac{1}{2}\sigma_J^2} (T-t) \right) e^{\hat{\mu}_X(n) + \frac{1}{2}\hat{\sigma}_X^2(n)(T-t)} \Phi(d_1), \tag{A.2}$$

$$\begin{aligned}
\frac{\partial V(t)}{\partial \sigma_J} &= e^{-r(T-t)} \sum_{n \geq 0} \frac{[\xi_J(T-t)]^n e^{-\xi_J(T-t)}}{n!} \\
&\quad \left(\sigma_J \left(n - \xi_J e^{\mu_J + \frac{1}{2}\sigma_J^2} (T-t) \right) e^{\hat{\mu}_X(n) + \frac{1}{2}\hat{\sigma}_X^2(n)(T-t)} \Phi(d_1) + K \phi(d_2) \frac{1}{\hat{\sigma}_X(n)} \frac{n\sigma_J}{\sqrt{T-t}} \right), \tag{A.3}
\end{aligned}$$

$$\begin{aligned}
\frac{\partial V(t)}{\partial \xi_J} &= e^{-r(T-t)} \sum_{n \geq 0} \frac{[\xi_J(T-t)]^n e^{-\xi_J(T-t)}}{n!} \\
&\quad \left(\bar{V}(n) \left[\frac{n}{\xi_J} - (T-t) \right] - \left(e^{\mu_J + \frac{1}{2}\sigma_J^2} - 1 \right) (T-t) e^{\hat{\mu}_X(n) + \frac{1}{2}\hat{\sigma}_X^2(n)(T-t)} \Phi(d_1) \right). \tag{A.4}
\end{aligned}$$

By the put-call parity it can easily be seen that the jump parameter sensitivities above hold for both call and put options.

In a similar fashion we can derive the following expression for the call option *delta* and *gamma* under the Merton jump-diffusion model:

$$\frac{\partial V(t)}{\partial S} = e^{-r(T-t)} \sum_{n \geq 0} \frac{[\xi_J(T-t)]^n e^{-\xi_J(T-t)}}{n!} \cdot e^{\hat{\mu}_X(n) - \log(S(t)) + \frac{1}{2} \hat{\sigma}_X^2(n)(T-t)} \Phi(d_1), \quad (\text{A.5})$$

$$\frac{\partial^2 V(t)}{\partial S^2} = e^{-r(T-t)} \sum_{n \geq 0} \frac{[\xi_J(T-t)]^n e^{-\xi_J(T-t)}}{n!} \cdot e^{\hat{\mu}_X(n) - \log(S(t)) + \frac{1}{2} \hat{\sigma}_X^2(n)(T-t)} \frac{\phi(d_1)}{S(t) \hat{\sigma}_X(n) \sqrt{T-t}}, \quad (\text{A.6})$$

The option pricing formula (A.1) contains an infinite sum of scaled Black-Scholes option prices, being a direct result of the jump size following a continuous distribution. This clearly shows that if one attempts to hedge the jump risk introduced by the model, one would theoretically need infinitely many options to do so, which is infeasible from a practical perspective.

Appendix A.2. Jump parameter impact on implied volatilities

Here we assess the impact of the jump parameters on the *Black-Scholes implied volatilities* σ_{imp} . This is done by varying the parameters μ_J , σ_J , and ξ_J one by one while keeping all the other parameters constant.

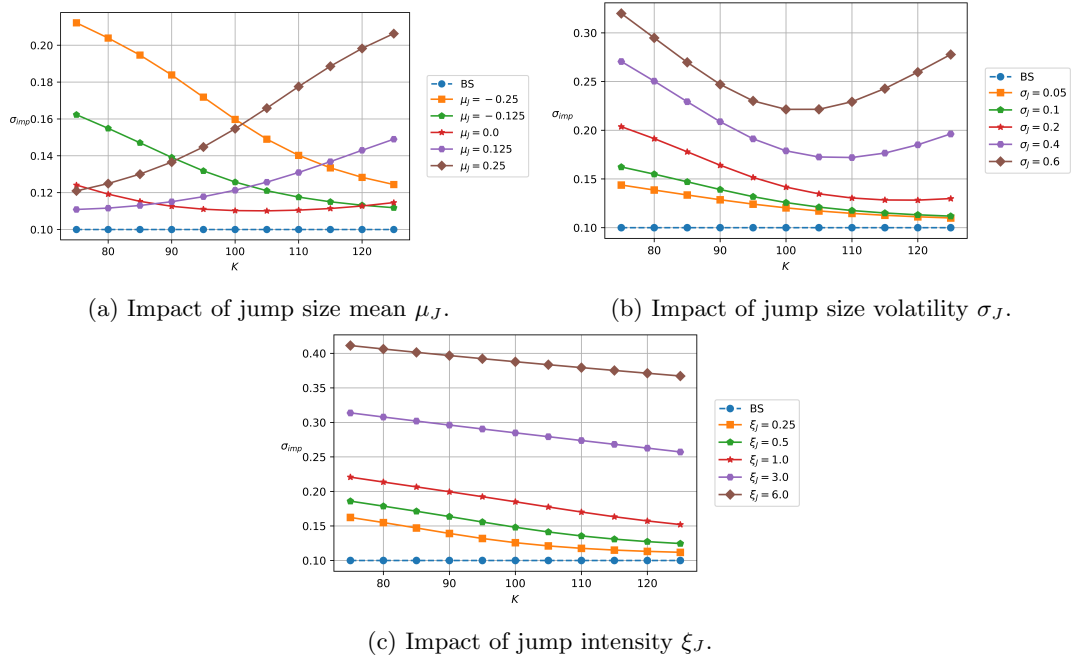


Figure A.12: Merton jump parameter impact on σ_{imp} . Parameters: $S(t_0) = 100$, $r = 0.05$, $\sigma = 0.1$, $t_0 = 0$, $T = 1$. Jump parameters base values: $\mu_J = -0.125$, $\sigma_J = 0.1$, $\xi_J = 0.25$. $\mu_J \in \{-0.25, -0.125, 0.0, 0.125, 0.25\}$, $\sigma_J \in \{0.05, 0.1, 0.2, 0.4, 0.6\}$, $\xi_J \in \{0.25, 0.5, 1.0, 3.0, 6.0\}$.

In Figure A.12a we observe that μ_J has a clear *level effect*. In addition the *slope*, i.e., *skew*, and direction of the slope are affected. For the simulations we will choose a negative value of μ_J , which implies that the stock will be likely to go down. The reason of this choice is that typically in the market we observe that OTM options are cheaper, which matches the higher likelihood of a downward jump in stock. From Figure A.12b we conclude that σ_J has an impact on both the level and the *curvature* of the implied volatility. This makes sense as a higher σ_J means more uncertainty, hence higher option prices, so also a higher σ_{imp} . The curvature effect can be observed by the OTM strike region exhibiting a more pronounced *hockey-stick* effect

which becomes larger as σ_J increases. Finally Figure A.12c tells us that ξ_J impacts the level only. For higher ξ_J , jumps will occur more frequently, introducing more uncertainty, resulting in higher σ_{imp} .

Appendix A.3. Convergence of number of terms in expansion

We have seen that the option price (A.1) as well as sensitivities (A.2-A.6) can be written as an infinite sum of scaled Black-Scholes option prices. The question arises how to approximate these infinite sums in a practical situation by means of a numerical implementation. Each of the quantities we need to compute contain the following weights in the infinite summation:

$$\frac{[\xi_J(T-t)]^n e^{-\xi_J(T-t)}}{n!}.$$

These weights appear to be exponentially decaying, indicating that in a numerical implementation the sum can simply be cut off at some point at which the desired accuracy is achieved.

As an example we cut off the option price at a *basis-point (bps)* level, i.e., 10^{-4} .

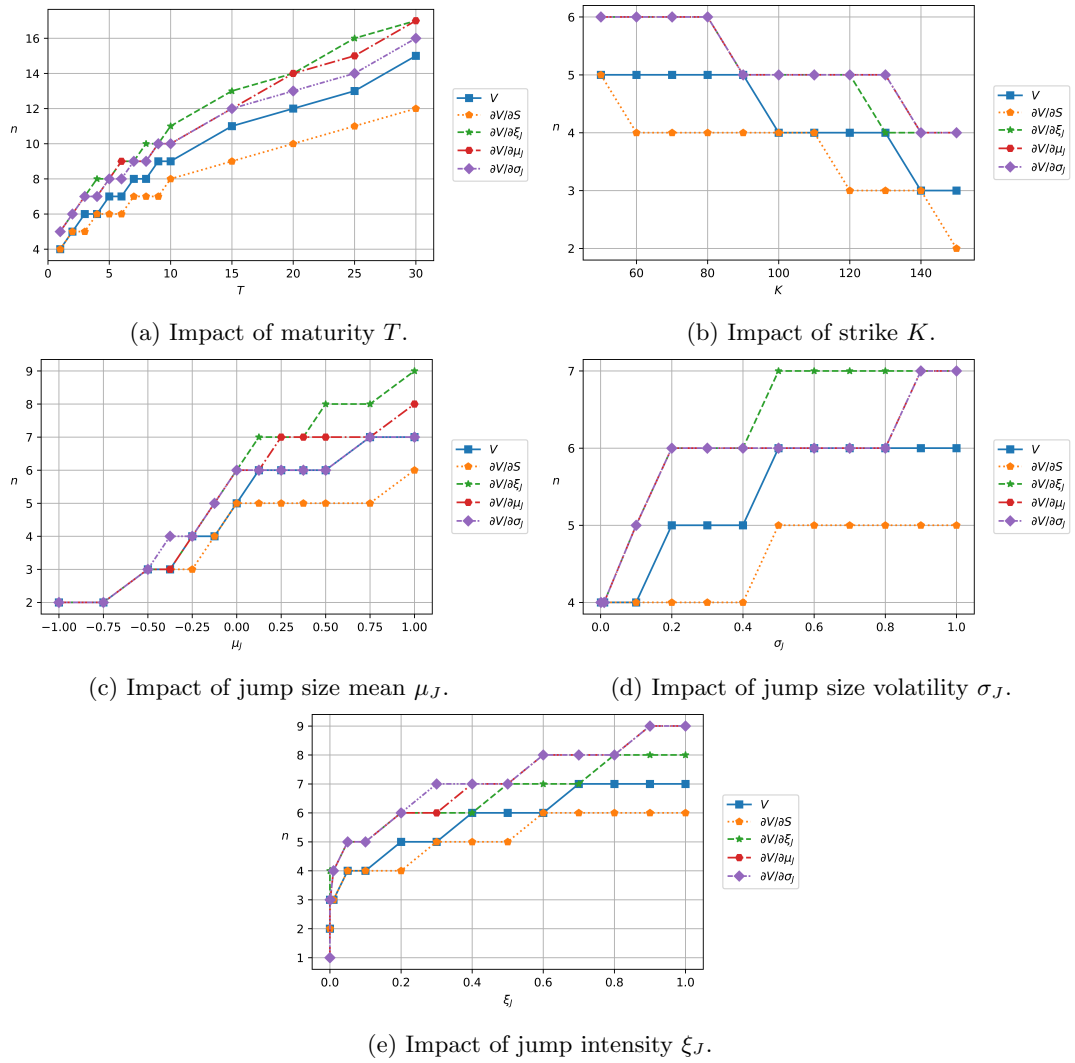


Figure A.13: Impact on number of terms in the Merton option price expansion. Tolerance 10^{-4} has been used to determine the cutoff point. Parameters: $t_0 = 0$, $T = 1$, $S(t_0) = 100$, $r = 0.1$, $\sigma = 0.2$, $K = 100$, $\mu_J = -0.125$, $\sigma_J = 0.1$, $\xi_J = 0.1$.

From the experiment in Figure A.13 we can conclude that for a chosen impact (T , K , μ_J , σ_J , ξ_J) all examined quantities (price, delta, jump parameter sensitivities) exhibit the same

pattern regarding the number of terms required to achieve the desired bps accuracy. Indeed, using a higher tolerance for the cutoff point yields a higher number of terms required in the expansion, see Figure A.14 where we cut off at 10^{-15} .

These results are in line with those presented by Boen on European rainbow option values under the two-asset Merton jump-diffusion model [17]. Boen derives a semi-closed analytical formula for European rainbow options, under the two-asset Merton jump-diffusion model. Depending on the size of $\xi_J(T-t)$ the number of terms used in the sum needs to be sufficiently large to guarantee accurate option prices. Convergence of this formula in the case of a European put-on-the-min option is illustrated.

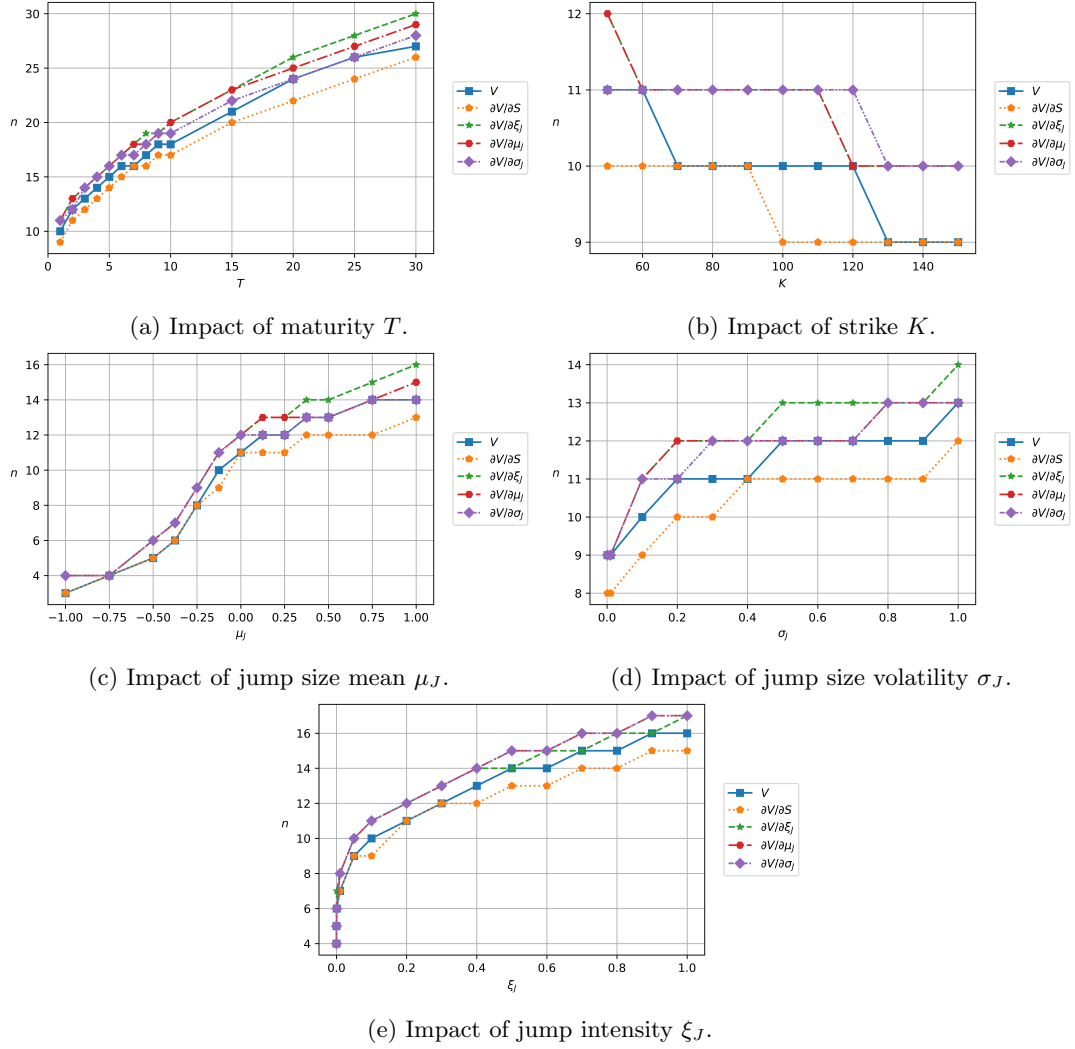


Figure A.14: Impact on number of terms in the Merton option price expansion. Tolerance 10^{-15} has been used to determine the cutoff point. Parameters: $t_0 = 0$, $T = 1$, $S(t_0) = 100$, $r = 0.1$, $\sigma = 0.2$, $K = 100$, $\mu_J = -0.125$, $\sigma_J = 0.1$, $\xi_J = 0.1$.

Appendix B. Variance analysis derivations

As is stated in Section 5.1.3, we derive an analytic expression for the mean and variance of $P\&L_P$ from Equation (5.6). But before that, we need the following two results. First,

$$\begin{aligned} S(t_k) &\stackrel{d}{=} S(t_{k-1})e^X, \\ X &= \left(r - \frac{1}{2}\sigma^2\right)[t_k - t_{k-1}] + \sigma\sqrt{t_k - t_{k-1}}Z \\ &\sim \mathcal{N}\left(\left(r - \frac{1}{2}\sigma^2\right)[t_k - t_{k-1}], \sigma^2[t_k - t_{k-1}]\right) =: \mathcal{N}(\mu_X, \sigma_X^2), \end{aligned} \quad (\text{B.1})$$

where $Z \sim \mathcal{N}(0, 1)$. Second, in a similar fashion as Equation (B.1) we write:

$$S(t_{k-1}) \stackrel{d}{=} S(t_0) \exp\left\{\left(r - \frac{1}{2}\sigma^2\right)[t_{k-1} - t_0] + \sigma\sqrt{t_{k-1} - t_0}\tilde{Z}\right\}, \quad (\text{B.2})$$

where $\tilde{Z} \sim \mathcal{N}(0, 1)$, independent of Z . Using Equation (B.2) and $\tau := T - t_{k-1}$ we write d_2 as:

$$\begin{aligned} d_2 &= \frac{\ln \frac{S(t_0)}{K} + (r - \frac{1}{2}\sigma^2)[T - t_0]}{\sigma\sqrt{\tau}} + \sqrt{\frac{t_{k-1} - t_0}{\tau}}\tilde{Z} \\ &\sim \mathcal{N}\left(\frac{\ln \frac{S(t_0)}{K} + (r - \frac{1}{2}\sigma^2)[T - t_0]}{\sigma\sqrt{\tau}}, \frac{t_{k-1} - t_0}{\tau}\right) =: \mathcal{N}(\mu_{d_2}, \sigma_{d_2}^2). \end{aligned}$$

Appendix B.1. Mean

We are interested in how $P\&L_P$ from Equation (5.6) is distributed conditional on the information known at today (t_0). First, look at the mean:

$$\mathbb{E}_{t_0}[P\&L_P(t_k)] \approx \mathbb{E}_{t_0}\left[\frac{Ke^{-r\tau}}{2\sigma\sqrt{\tau}}[e^X - 1]^2\phi(d_2)\right] = \frac{Ke^{-r\tau}}{2\sigma\sqrt{\tau}}\mathbb{E}_{t_0}\left[[e^X - 1]^2\right]\mathbb{E}_{t_0}[\phi(d_2)], \quad (\text{B.3})$$

where we use the independency of $[e^X - 1]^2$ and $\phi(d_2)$ due to the independent increments. The first expectation from Equation (B.3) can be written as:

$$\begin{aligned} \mathbb{E}_{t_0}\left[[e^X - 1]^2\right] &= \text{Var}_{t_0}(e^X - 1) + (\mathbb{E}_{t_0}[e^X - 1])^2 \\ &= (e^{\sigma_X^2} - 1)e^{2\mu_X + \sigma_X^2} + (e^{\mu_X + \frac{1}{2}\sigma_X^2} - 1)^2, \end{aligned} \quad (\text{B.4})$$

where we use the lognormality of e^X . The second expectation can be written as:

$$\mathbb{E}_{t_0}[\phi(d_2)] = \frac{\mathbb{E}_{t_0}[e^{-\frac{1}{2}d_2^2}]}{\sqrt{2\pi}} = \frac{e^{-\frac{\mu_{d_2}^2}{2(1+\sigma_{d_2}^2)}}}{\sqrt{2\pi}\sqrt{1+\sigma_{d_2}^2}}, \quad (\text{B.5})$$

where we use the fact that d_2^2 follows $\sigma_{d_2}^2$ times a non-central chi-squared distribution with one degree of freedom ($k = 1$), and with non-centrality parameter $\lambda = \frac{\mu_{d_2}^2}{\sigma_{d_2}^2}$, i.e., $d_2^2 \sim \sigma_{d_2}^2\chi^2\left(1, \frac{\mu_{d_2}^2}{\sigma_{d_2}^2}\right)$. Using results (B.4) and (B.5) allows us to rewrite Equation (B.3) as:

$$\mathbb{E}_{t_0}[P\&L_P(t_k)] \approx \frac{Ke^{-r\tau}}{2\sigma\sqrt{\tau}}\frac{e^{-\frac{\mu_{d_2}^2}{2(1+\sigma_{d_2}^2)}}}{\sqrt{2\pi}\sqrt{1+\sigma_{d_2}^2}}\left(\left(e^{\sigma_X^2} - 1\right)e^{2\mu_X + \sigma_X^2} + \left(e^{\mu_X + \frac{1}{2}\sigma_X^2} - 1\right)^2\right). \quad (\text{B.6})$$

Appendix B.2. Variance

For the variance of $P\&L_P$ from Equation (5.6) we have:

$$\text{Var}_{t_0} (P\&L_P(t_k)) = \mathbb{E}_{t_0} \left[(P\&L_P(t_k))^2 \right] - (\mathbb{E}_{t_0} [P\&L_P(t_k)])^2, \quad (\text{B.7})$$

where the second term can be computed using Equation (B.6). By the independent increment argument, the first term in Equation (B.7) can be written as:

$$\begin{aligned} \mathbb{E}_{t_0} \left[(P\&L_P(t_k))^2 \right] &\approx \mathbb{E}_{t_0} \left[\left(\frac{K e^{-r\tau}}{2\sigma\sqrt{\tau}} [e^X - 1]^2 \phi(d_2) \right)^2 \right] \\ &= \frac{K^2 e^{-2r\tau}}{4\sigma^2\tau} \mathbb{E}_{t_0} \left[[e^X - 1]^4 \right] \mathbb{E}_{t_0} \left[(\phi(d_2))^2 \right]. \end{aligned} \quad (\text{B.8})$$

For the first expectation in Equation (B.8) we write:

$$\begin{aligned} \mathbb{E}_{t_0} \left[[e^X - 1]^4 \right] &= \mathbb{E}_{t_0} [e^{4X} - 4e^{3X} + 6e^{2X} - 4e^X + 1] \\ &= e^{4\mu_X + \frac{16}{2}\sigma_X^2} - 4e^{3\mu_X + \frac{9}{2}\sigma_X^2} + 6e^{2\mu_X + \frac{4}{2}\sigma_X^2} - 4e^{\mu_X + \frac{1}{2}\sigma_X^2} + 1, \end{aligned} \quad (\text{B.9})$$

using the properties of the moment generating function of X . The second expectation in Equation (B.8) can be written as:

$$\mathbb{E}_{t_0} \left[(\phi(d_2))^2 \right] = \frac{\mathbb{E}_{t_0} [e^{-d_2^2}]}{2\pi} = \frac{e^{-\frac{\mu_{d_2}^2}{1+2\sigma_{d_2}^2}}}{2\pi\sqrt{1+2\sigma_{d_2}^2}}, \quad (\text{B.10})$$

where we once more use that d_2^2 follows $\sigma_{d_2}^2$ times a non-central chi-squared distribution with parameters as stated before. Results (B.9) and (B.10) allow us to rewrite Equation (B.8) as:

$$\begin{aligned} \mathbb{E}_{t_0} \left[(P\&L_P(t_k))^2 \right] &\approx \frac{K^2 e^{-2r\tau}}{4\sigma^2\tau} \frac{e^{-\frac{\mu_{d_2}^2}{1+2\sigma_{d_2}^2}}}{2\pi\sqrt{1+2\sigma_{d_2}^2}} \\ &\quad \left(e^{4\mu_X + \frac{16}{2}\sigma_X^2} - 4e^{3\mu_X + \frac{9}{2}\sigma_X^2} + 6e^{2\mu_X + \frac{4}{2}\sigma_X^2} - 4e^{\mu_X + \frac{1}{2}\sigma_X^2} + 1 \right). \end{aligned} \quad (\text{B.11})$$

Using the results from Equations (B.6) and (B.11) in Equation (B.7) yields:

$$\text{Var}_{t_0} (P\&L_P(t_k)) \approx \frac{K^2 e^{-2r\tau}}{8\pi\sigma^2\tau} \left[f(\mu_X, \sigma_X) \cdot \frac{e^{-\frac{\mu_{d_2}^2}{1+2\sigma_{d_2}^2}}}{\sqrt{1+2\sigma_{d_2}^2}} - g(\mu_X, \sigma_X) \cdot \frac{e^{-\frac{\mu_{d_2}^2}{1+\sigma_{d_2}^2}}}{1+\sigma_{d_2}^2} \right], \quad (\text{B.12})$$

where

$$f(\mu_X, \sigma_X) := e^{4\mu_X + \frac{16}{2}\sigma_X^2} - 4e^{3\mu_X + \frac{9}{2}\sigma_X^2} + 6e^{2\mu_X + \frac{4}{2}\sigma_X^2} - 4e^{\mu_X + \frac{1}{2}\sigma_X^2} + 1, \quad (\text{B.13})$$

$$g(\mu_X, \sigma_X) := \left((e^{\sigma_X^2} - 1) e^{2\mu_X + \sigma_X^2} + (e^{\mu_X + \frac{1}{2}\sigma_X^2} - 1)^2 \right)^2. \quad (\text{B.14})$$

Appendix C. Desk structure and flow of cash

The simulation is illustrated by a series of schematic drawings that indicate the flow of cash and instruments. First, in Appendix C.1, we consider the case without CCR to get a basic understanding. In Appendix C.2, CCR is introduced, and the trading desk and xVA desk are represented as a single entity, referred to as the trading desk. Finally, in Appendix C.3, we remove this assumption by examining the internal exchange of cash-flows and products between the desks. In all figures to follow, dotted lines indicate flows of cash, hence this relates

to wealth accounts w , w^{trading} , and w^{xVA} . Furthermore, solid lines indicate the exchange of a product/asset, hence this relates to portfolios Π , Π^{trading} , and Π^{xVA} . Values are seen from the perspective of the desks, i.e., an arrow away from a desk indicates the desk needs to pay and an arrow towards a desk indicates the desk receives. We assume that the wealth account at time t_{k-1} is positive, in the sense that this can be seen as a deposit with the Treasury department for which interest is received.¹²

Appendix C.1. Case without CCR

At this stage the xVA desk is not involved as we assume no xVAs are required. Here

$$\eta_1(t) = -\Delta(t) = -\frac{\partial V(t)}{\partial S}. \quad (\text{C.1})$$

At t_0 , see Figure C.15, the option is bought from the counterparty (blue lines) and the Black-Scholes delta hedge (C.1) is constructed (red lines).

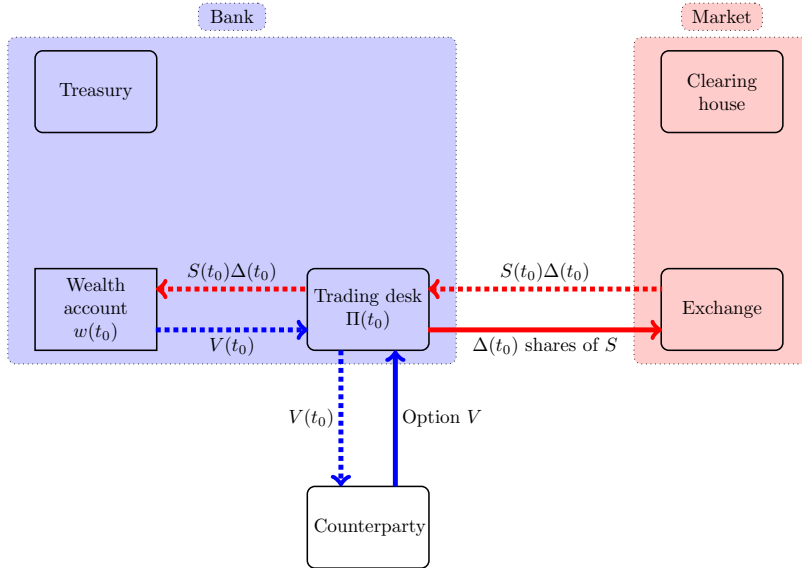


Figure C.15: Case without CCR, situation at t_0 . The blue lines correspond to the trade; the red lines correspond to the hedge.

Then for $t_0 < t_k < t_K$, see Figure C.16, interest on the wealth account is received from the Treasury department (teal lines) and the hedge is rebalanced (red lines).

Finally, the situation maturity t_K is displayed in Figure C.17. We first again receive interest (teal lines), then close the hedge (red lines) and settle the payoff of the option in cash (blue lines).

Appendix C.2. Case with CCR, single desk within the bank

Assume that the trading desk and xVA desk are represented as a single entity, still referred to as the trading desk. Here

$$\eta_1(t) = -\hat{\Delta}(t) = -\frac{\partial V(t)}{\partial S} [1 - (1 - R) \text{PD}(t, t_K)], \quad (\text{C.2})$$

meaning that also the market-risk component of the CVA is hedged in the market.

Initially at t_0 , see Figure C.18, the risky option V_1 is bought from the counterparty (blue lines). As in the previous case, we construct a hedge (red lines), but now with a position that takes into account the hedging of CVA, see Equation (C.2).

¹²In the case that $w(t_{k-1})$ is negative we have to pay interest to the Treasury desk on the borrowed amount and the flows between the Treasury department and wealth account would be in the opposite direction.

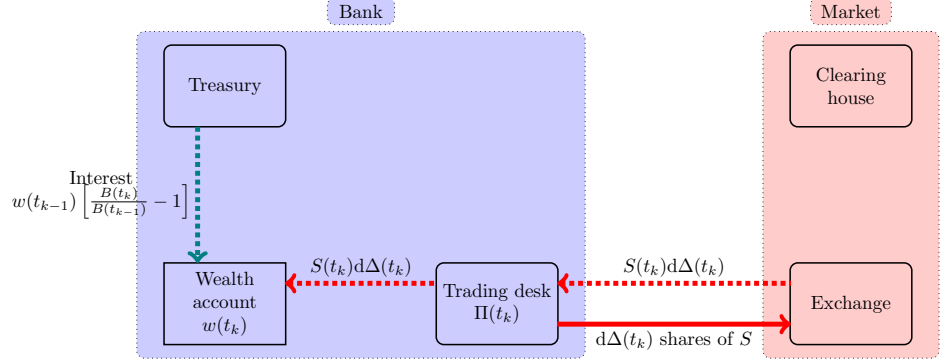


Figure C.16: Case without CCR, situation at $t_0 < t_k < t_K$. The red lines correspond to the hedge; the teal lines correspond to the interest.

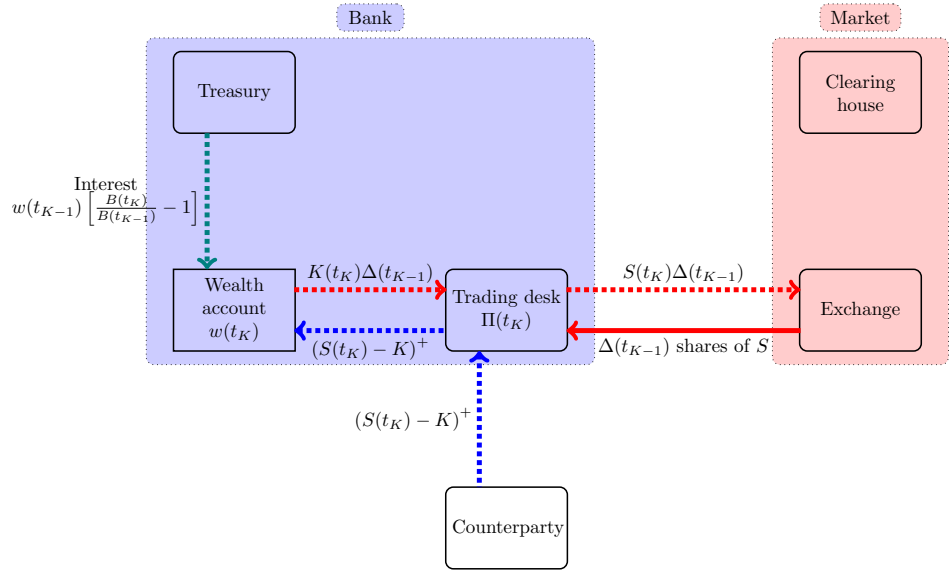


Figure C.17: Case without CCR, situation at t_K . The blue lines correspond to the trade; the red lines correspond to the hedge; the teal lines correspond to the interest.

For $t_0 < t_k < t_K$ if there is no default, we rebalance our hedge as before and receive interest on the wealth account. If a default does occur, see Figure C.19, the risk-free closeout takes place (brown lines) and the same risk-neutral option is bought from the clearing house (violet lines). ¹³ As always, we receive interest (teal lines). Regarding the hedge (red lines), there we close the hedge that takes into account the CVA, see Equation (C.2), and construct a new hedge for the option bought from the clearing house. This new hedge is equivalent to the Black-Scholes hedge for the risk-free case in Equation (C.1).

The situation at maturity, see Figure C.20, is then the same as for the case without CCR, apart from the payoff of the option now being settled with the clearing house rather than the counterparty.

¹³Here we assume the default takes place before maturity. The case of default at maturity is not discussed for sake of brevity. The remaining case naturally extends from the demonstrated material.

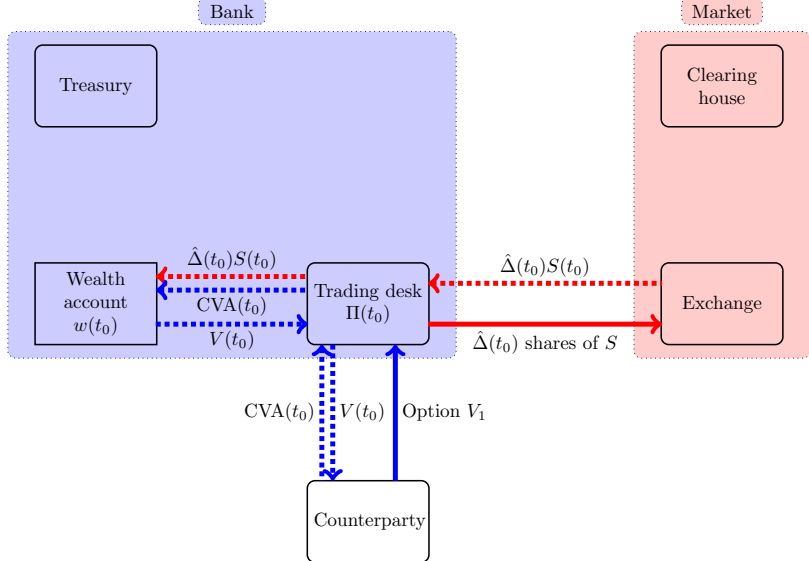


Figure C.18: Case with CCR, single desk within the bank, situation at t_0 . The blue lines correspond to the trade; the red lines correspond to the hedge.

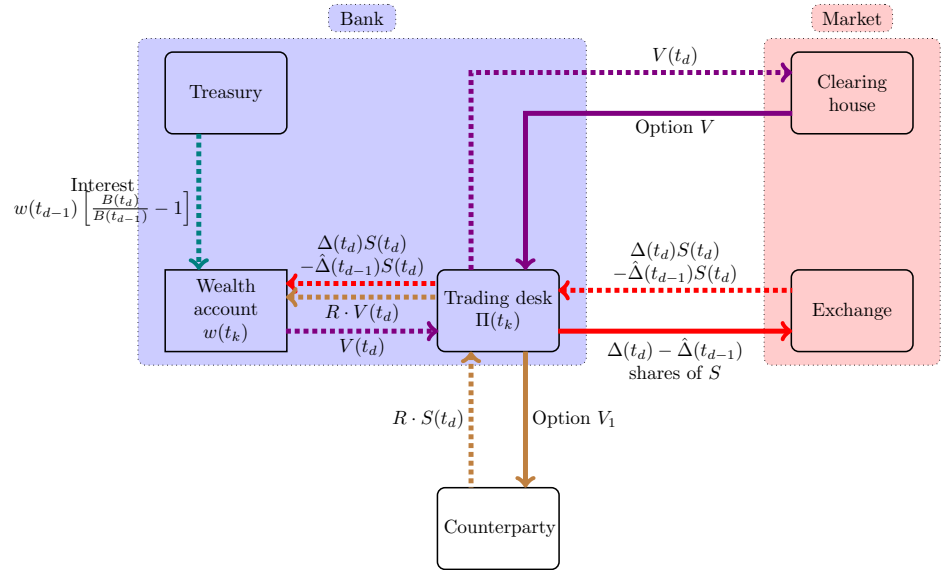


Figure C.19: Case with CCR, single desk within the bank, situation at $t_0 < \tau = t_d < t_K = T$. The red lines correspond to the hedge; the teal lines correspond to the interest; the brown lines correspond to the default; the violet lines correspond to the new trade entered upon default.

Appendix C.3. Case with CCR, separate trading desk and xVA desk within the bank

We now remove the assumption of a single desk, and examine the internal exchange of cash-flows and products between the trading desk and xVA desk. Here

$$\eta_1(t) = \underbrace{-\frac{\partial V(t)}{\partial S}}_{-\Delta(t)} + \underbrace{\frac{\partial V(t)}{\partial S}(1 - R) \text{PD}(t, t_K)}_{-\bar{\Delta}(t)},$$

meaning that also the market-risk component of the CVA is hedged in the market.

Initially, the situation at t_0 is displayed in Figure C.21, where the positions in trading and hedging instruments are assumed. Note the transfer of the CVA between the trading and xVA

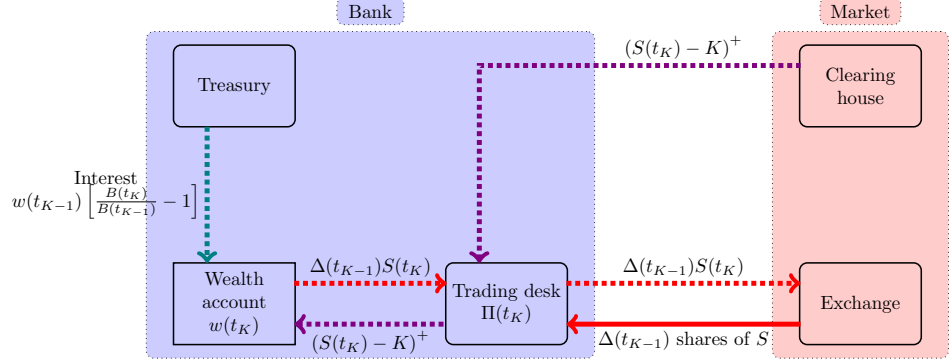


Figure C.20: Case with CCR, single desk within the bank, situation at t_K . The red lines correspond to the hedge; the teal lines correspond to the interest; the violet lines correspond to the new trade entered upon default.

desk, indicating that the trading desk manages the risk-free component of the transaction, whereas the xVA desk takes responsibility for the CVA.

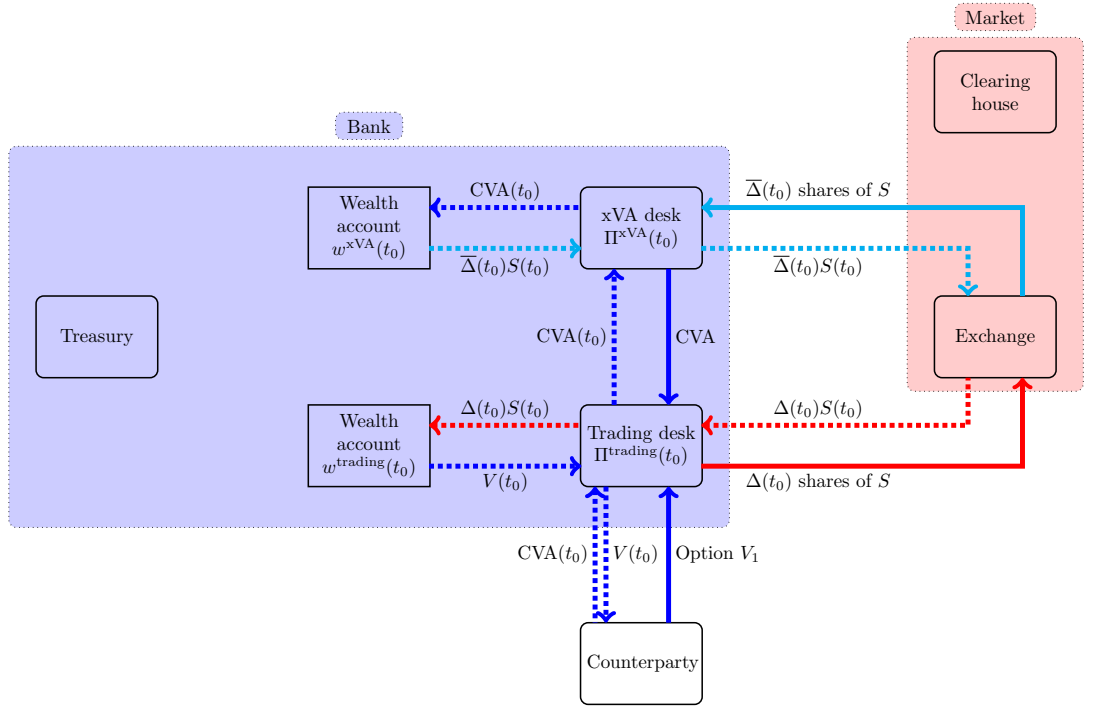


Figure C.21: Case with CCR, separate trading desk and xVA desk within the bank, situation at t_0 . The blue lines correspond to the trade; the red lines correspond to the hedge; the cyan lines correspond to the CVA hedge.

At $t_0 < t_k < t_K$, if there is no default, both desks rebalance their hedging positions and receive interest on their wealth account. In case of a default at $t_0 < \tau = t_d < t_K$, see Figure C.22, a risk-free closeout takes place between the bank and the counterparty. Furthermore, the xVA desk enters the same risk-free contract V with a clearing house and closes its hedging position on the CVA. The xVA desk then gives the new contract V to the trading desk, so that they are immune to the default. The ‘damage’ of the default is thus visible at the xVA desk level, which is precisely the place handling this risk.

Finally, Figure C.23 represents the situation at t_K , at which the option payoff is settled in cash, and the trading desk closes its hedging positions. The output metrics as introduced in Section 3.1 can be carefully analyzed to draw conclusions about the hedging strategy used.

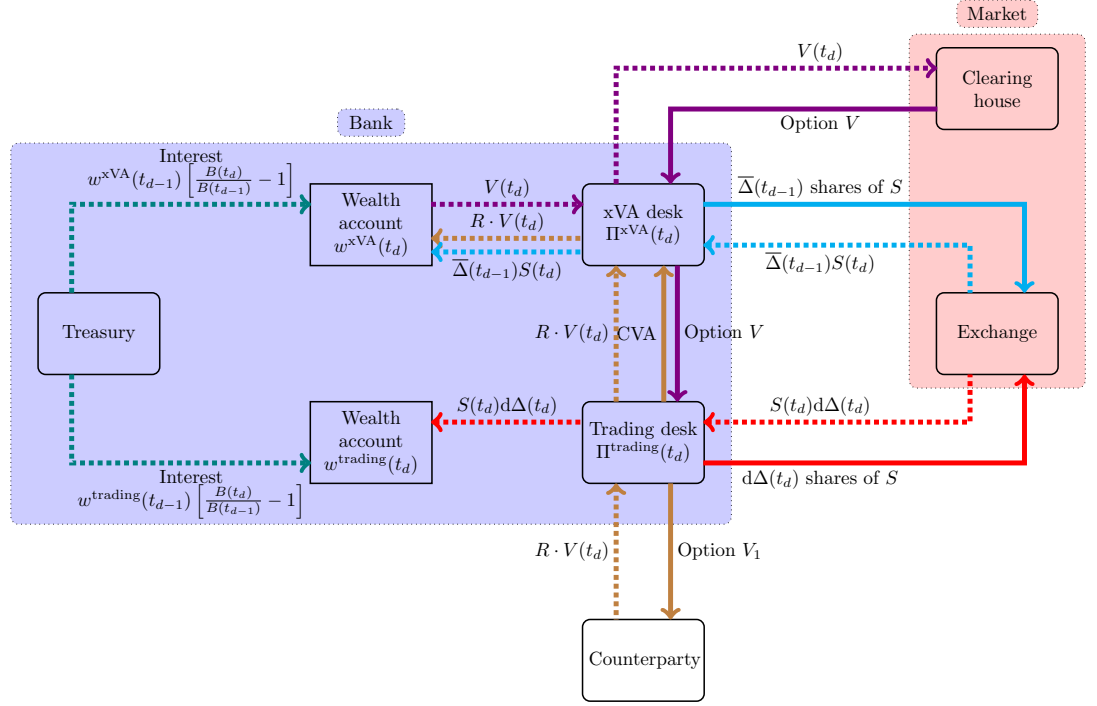


Figure C.22: Case with CCR, separate trading desk and xVA desk within the bank, situation at $t_0 < \tau = t_d < t_K$. The red lines correspond to the hedge; the cyan lines correspond to the CVA hedge; the teal lines correspond to the interest; the brown lines correspond to the default; the violet lines correspond to the new trade entered upon default.

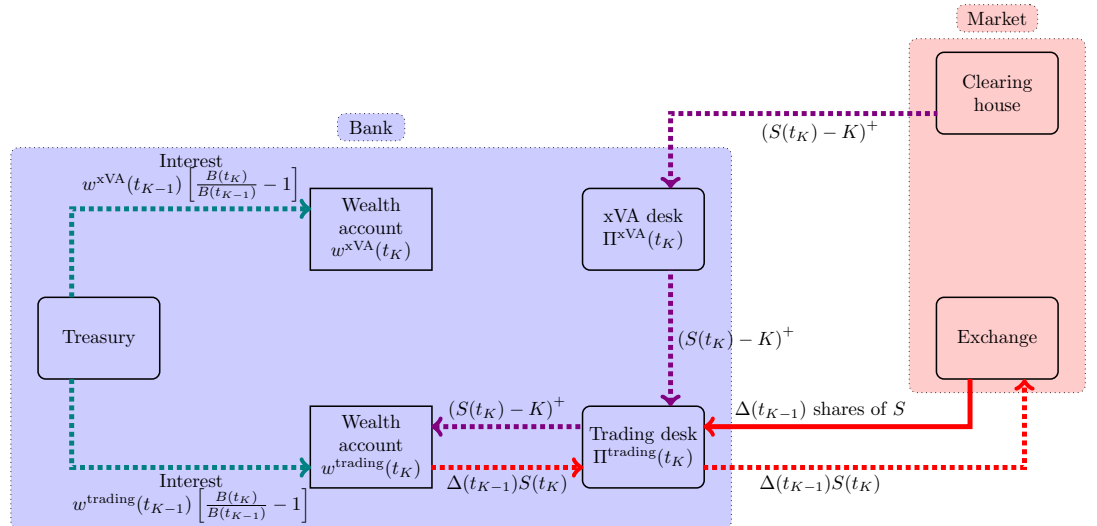


Figure C.23: Case with CCR, separate trading desk and xVA desk within the bank, situation at t_K . The red lines correspond to the hedge; the teal lines correspond to the interest; the violet lines correspond to the new trade entered upon default.